



# TECHNICAL NOTE

## D-1314

BOILING HEAT TRANSFER TO LIQUID HYDROGEN  
AND NITROGEN IN FORCED FLOW

By James P. Lewis, Jack H. Goodykoontz,  
and John F. Kline

Lewis Research Center  
Cleveland, Ohio

NATIONAL AERONAUTICS AND SPACE ADMINISTRATION  
WASHINGTON

September 1962

ERRATA

NASA TECHNICAL NOTE D-1314

By James P. Lewis, Jack H. Goodykoontz,  
and John F. Kline

September 1962

Page 19, equation (A11): The symbol  $R$  should be  $R_o$ .

Page 52, figure 17: The abscissa scale label should be Wall superheat,  $t_{w,i} - t_{sat}$ ,  $^{\circ}R$  instead of Water superheat,  $t_{w,i} - t_{sat}$ ,  $^{\circ}R$ .

## NATIONAL AERONAUTICS AND SPACE ADMINISTRATION

## TECHNICAL NOTE D-1314

BOILING HEAT TRANSFER TO LIQUID HYDROGEN  
AND NITROGEN IN FORCED FLOWBy James P. Lewis, Jack H. Goodykoontz,  
and John F. Kline

## SUMMARY

Boiling heat transfer to liquid hydrogen and nitrogen was investigated experimentally. Results are presented from a study of bulk boiling inside a cylindrical tube under vertically upward forced-flow conditions. A 0.555-inch-inside-diameter and  $16\frac{1}{8}$ -inch-long electrically heated stainless-steel tube was used. The range of variables studied for hydrogen were mass velocity of 2850 to 17,000 pounds per hour per square foot, local heat flux of 3600 to 40,000 Btu per hour per square foot, inlet pressure of 30 to 74 pounds per square inch absolute, and inlet subcooling of  $0^{\circ}$  to  $9^{\circ}$  R. Nitrogen test conditions were mass velocity of 15,000 to 56,000 pounds per hour per square foot, local heat flux of 2300 to 40,000 Btu per hour per square foot, inlet pressure of 47 to 56 pounds per square inch absolute, and inlet subcooling of  $1^{\circ}$  to  $6^{\circ}$  R.

The axial distribution of the tube-wall temperatures is presented. A transition in the type of boiling heat transfer was obtained. The critical heat flux corresponding to this transition was determined over a range of flow and heating rates and local qualities. At specific combinations of flow and transition location, a range of critical-heat-flux values was obtained and maximum values were determined. The maximum critical heat flux increased with increasing fluid-flow rate and decreased with increasing length of tube before transition. Similar variations of the maximum critical heat flux have been reported for water. The tube-inner-wall temperatures upstream of transition were essentially uniform and were only slightly greater than the fluid saturation temperature. The wall-temperature profiles downstream of transition generally resembled those obtained in film-boiling studies and appeared to be strongly dependent upon local quality at the point of transition. Maximum wall temperatures of  $900^{\circ}$  and  $1800^{\circ}$  R were obtained with hydrogen and nitrogen, respectively. Fluctuations of pressure, flow rate, and temperature occurred during some of the boiling tests. Under some conditions, maximum critical-heat-flux values were attained during steady-state operation with fluctuations. In other cases the fluctuations became uncontrolled, and critical-flux values less than the maximum values were obtained upon restabilization of the test conditions. No measurable pressure drop across the test section was obtained at any condition.

## INTRODUCTION

Liquid hydrogen has been proposed for use in several advanced propulsion systems. In these systems, hydrogen may be used both as a propellant and as a coolant. The low boiling point of hydrogen and the desirability of storing it in the liquid state in addition to the requirements of some systems for gaseous hydrogen necessitate a knowledge of two-phase flow and heat transfer for hydrogen. Information is especially desired for boiling heat transfer of hydrogen under forced-flow, confined-geometry conditions. In addition, the wide variance of the physical properties of hydrogen from those of more conventional fluids make it attractive as a test fluid in research directed towards a more complete understanding of the general problem of boiling heat transfer.

Information in the literature concerning boiling heat transfer, primarily for the case of pool (or pot) boiling and usually for conventional fluids, such as water and alcohols, is extensive. Present thinking with respect to pool boiling and related investigations with hydrogen are summarized in reference 1. Pool boiling is characterized by three distinct modes of boiling, namely, nucleate, transition, and film boiling. Analytical and empirical relations between the heat flux (or heat-transfer coefficient) and the wall- to fluid-temperature difference have been obtained for pool boiling. Pool boiling also exhibits a distinctive value of heat flux obtained at the boundary between the nucleate and transition boiling regions that has been variously termed maximum nucleate flux, departure from nucleate boiling (DNB), or burnout heat flux. Analytical and experimental correlations of the maximum nucleate flux with fluid properties and test operating variables have been made with varying degrees of success (ref. 1).

For the case of forced flow in confined geometries, the current understanding of boiling heat transfer is much more limited, especially for the case of net vapor generation. Again, considerable data have been obtained and several correlations have been proposed (refs. 2 to 6). Much of the available data are incompletely presented or contradictory, and the correlations, which successfully relate the results of a single study, have not been successful when applied to other tests or fluids of widely differing properties. The experimental data of several investigations (refs. 2 to 4) have indicated the existence of a critical heat flux, which somewhat resembles the maximum nucleate flux obtained in pool boiling, in that a well defined reduction in the heat-transfer coefficient is obtained. Some data of this type that resemble the usual results obtained for pool boiling were obtained in limited tests of boiling hydrogen (ref. 7). Data were obtained in reference 8 for hydrogen for the region that might be termed film boiling in tubes with forced flow. For the investigations of boiling heat transfer with forced flow in confined geometries, there is a wide variation in the assumptions regarding the physical nature of the heat-transfer process and in the definition of the critical heat flux.

Because of the aforementioned limitations of present knowledge, a program was initiated at the Lewis Research Center to investigate boiling heat transfer to liquid hydrogen under conditions of forced flow inside a vertical tube. The principal objective of the investigation was to determine in engineering terms the effect of the operating variables (flow rate, pressure, liquid inlet subcooling, heating rate, and tube geometry) on the mode of heat transfer and their relation to the value of the critical heat flux. The program was directed towards conditions resulting in net vapor generation. In addition, information on flow instability and its effect on heat transfer were desired.

The test apparatus consisted of a pressure-fed, once-through system with an electrically heated vertical tube of 0.555-inch inside diameter and  $16\frac{1}{8}$ -inch length. Both subcooled liquid para-hydrogen and liquid nitrogen flowed through the tube in vertical upflow. The range of variables investigated was limited to the following:

	Hydrogen	Nitrogen
Mass velocity, lb/(hr)(sq ft)	2850 to 17,000	15,000 to 56,000
Local heat flux, Btu/(hr)(sq ft)	3600 to 40,000	2300 to 40,000
Liquid inlet subcooling, °R	0 to 9	1 to 6
Inlet pressure, lb/sq in. abs	30 to 74	47 to 56

Tube-exit qualities ranged from essentially 0 to 1.0 (with superheat), and transition from a relatively high to a lower value of heat-transfer coefficient occurred over a range of axial locations from tube entrance to exit. A few tests were made with cold hydrogen gas flowing through a heated tube. The results obtained from the investigation are presented in tabular and graphical form.

## APPARATUS

### General Arrangement

The test equipment included a liquid-supply Dewar, a controlled source of pressurizing gas, a flash cooler to subcool inlet test liquid, the test section and electric power supply, inlet and exit control valves, a vaporizer, an orifice-type flowmeter, and vent, pressure relief, and purge systems (fig. 1). In practically every case, the test liquids (para-hydrogen and nitrogen) were pressurized by their own gases. Gaseous helium was used for system purging and inerting. The vaporizer was used to ensure that only a fully vaporized product would pass through the flow orifice. All fluid lines from the supply Dewar to a point past the end of the test section were insulated with a vacuum jacket.

### Test Section

The test-section assembly consisted of the electrically heated tube, inlet and outlet chambers, a vacuum jacket, and test instrumentation (fig. 2). The tube was made of type 304 stainless steel with a 0.555-inch inside diameter and a 0.035-inch-thick wall. As indicated in figure 2, the effective heated length of the tube was  $16\frac{1}{8}$  inches, measured between the inner faces of the end flanges. All distances along the tube from the tube inlet were measured from the downstream side of the inlet flange. The actual inlet end of the tube extended  $1/2$  inch upstream of this point. The inlet chamber consisted of a  $1\frac{1}{2}$ -inch-inside-diameter stainless-steel cylinder attached to the inlet flange. The inlet chamber, which was lined with  $1/8$ -inch-thick thermal insulation, was designed to provide a low-velocity plenum at the test-section entrance and to minimize heat leakage from the heated test section to the incoming liquid. Two copper bus bars, diametrically opposite, were connected between the test-section inlet flange and the bottom flange of the vacuum jacket, which also served as the ground side of the electrical circuit. These bus bars were 4 inches long with a cross section of  $1/8$  by 1 inch. The outlet chamber was designed to minimize heat losses from the tube, to provide an electrically insulated, low-electrical-resistance connection to the tube, and to provide a thermally insulated mixing chamber, in which the test fluid could come into thermal and phase equilibrium. The outlet chamber contained an inner liner consisting of stainless steel and Teflon. This liner, which was not attached directly to the tube, was designed to allow cool gas to accumulate between it and the outer shell and thus to act as thermal insulation. The outlet section was connected to a 1-inch-outside-diameter copper tube that passed through the vacuum jacket and was electrically isolated from it. Two conically shaped mixing screens were placed in the outlet section. The vacuum jacket around the test-section assembly consisted of stainless-steel flanges with O-ring seals, a  $3\frac{1}{2}$ -inch-diameter Lucite tube, and an aluminum-foil radiation shield.

### Flash Cooler

The flash cooler shown in figure 1 was provided to supply subcooled liquid to the test section. The cooler consisted basically of three concentric tubes. The flow of the liquid to the test section was brought through the small innermost tube. Some liquid was allowed to pass into the annular space around the inner tube through bleed holes at various points along the length of the subcooler. The pressure in this annulus was maintained intermediate between atmospheric pressure and the supply Dewar pressure by a throttle valve. The liquid entering the annular

space vaporized because of the drop in pressure and thus cooled the inner supply tube. The inner tube had a 0.38-inch outside diameter with a 0.032-inch wall. Stainless-steel rods, 1/4 inch in diameter, were inserted into the inner tube to promote cooling of the supply liquid. The outer annular space provided a vacuum jacket for thermal insulation.

### Electric Power Supply

The tube was heated by alternating current supplied through a  $2\frac{1}{2}$ -kilowatt, 60-cycle transformer with a maximum current rating of 500 amperes. The power to the test section was controlled by a variable autotransformer in the primary circuit. The current to the test section was measured by a laboratory-quality ammeter connected to a current transformer with a ratio of 100. Voltage drops across the tube at various locations were measured with a Ballantine vacuum-tube voltmeter.

### Instrumentation

Instrumentation was provided to measure the inlet and the exit fluid bulk temperatures, the tube-wall temperatures, the inlet-fluid pressure, and the test-fluid flow rate.

Fluid temperatures. - The fluid bulk temperatures were measured by carbon resistors in the inlet and the exit of the test section (see fig. 2). The carbon resistors at the test-section outlet were located both above and below the mixing screens. The carbon resistors were hermetically sealed in a protective sheath about 0.1 inch in diameter by 0.2 inch long. The carbon resistors acted as one arm of a bridge circuit, the output of which was recorded on a self-balancing potentiometer. The slope of the temperature-resistance curve was obtained in a laboratory calibration and was essentially invariant. Shifts of the curve occurred, however, that required daily adjustment with a trimming resistance at a known temperature condition. The fluid temperature at the orifice flowmeter was measured with a copper-constantan thermocouple. The overall accuracy of the fluid bulk temperatures is estimated at approximately  $\pm 0.5^\circ \text{R}$ .

Wall temperatures. - The temperatures of the tube wall and of adjacent sections were obtained with copper-constantan thermocouples. The thermocouples were soldered to the outside of the tube wall and the leads were wrapped around the tube several times and were finally wrapped with glass-fiber tape. The tube-wall thermocouples were positioned in one longitudinal plane and their axial locations are given in table I. The positions of the thermocouples that were installed on the inlet section, the outlet section, and the ground bus are also given in table I. These thermocouples were used to monitor the flow of heat to and from the test section.

The constantan wire from each thermocouple junction was led without interruption to individual reference junctions located in a liquid-nitrogen bath at atmospheric pressure. Copper leads led from the bath to a manual selector switch. The thermocouple voltage was bucked by a 1-millivolt voltage to obtain positive values, and the resultant signal was recorded on a self-balancing potentiometer. The calibration of the thermocouples was determined from the National Bureau of Standards calibration (ref. 9) and laboratory calibration checks. The calibration indicated a very low sensitivity for the copper-constantan thermocouples near liquid-hydrogen temperatures. Wall temperatures, however, were obtained from approximately 40° to 1800° R. Above 1200° R, an extrapolation of the curve of reference 9 was used. The sensitivity and accuracy of the thermocouple readings are indicated by the following table:

	Liquid-hydrogen temperature (45° R)	Liquid-nitrogen temperature (160° R)	Room tempera- ture (530° R)
Sensitivity, mv/°R	0.004	0.01	0.022
Chart reading limit, mv	0.01 to 0.02	0.01 to 0.02	0.01 to 0.02
Chart reading limit, °R	2.5 to 5	1 to 2	0.5 to 1

The thermocouple calibration points also showed a scatter of approximately  $\pm 3^\circ$  R at liquid-hydrogen temperatures and  $\pm 1^\circ$  R at liquid-nitrogen temperatures. Approximately the same scatter was obtained from the actual tube-wall thermocouples during no-heat runs. The tube-wall thermocouples were attached to the outside of the tube wall. The temperature of interest, however, is that of the inner surface. An analysis and computation of the temperature drop through the tube wall is given in appendix A for the case of negligible axial temperature gradients. This analysis indicates wall drops of up to 20° R for liquid-hydrogen conditions and up to 7° R for liquid-nitrogen conditions over the range of the test heat fluxes.

Pressure. - The fluid pressures were sensed with strain-gage-type transducers and were continuously recorded on a high-speed recording potentiometer (0.3-sec full-scale travel). Pressure was sensed at the test-section inlet (see fig. 2) by a transducer having a range of 0 to 100 pounds per square inch absolute and an overall accuracy of  $\pm 0.5$  percent of full scale. Initially a differential pressure transducer was installed to measure the pressure drop across the test section. Since no measurable pressure drop was obtained at the largest flow and vaporization conditions, the downstream pressure tap was removed to aid in eliminating flow and pressure oscillations. The fluid pressure far downstream of the tube exit (upstream of the exit control valve) was monitored on a visual gage but showed no significant drop from the test-section inlet pressure. The pressure in the flash cooler was also sensed by a strain-gage transducer.



E-878

Flow rate. - The test-fluid flow rate was measured by a sharp-edge orifice downstream of the vaporizer. The vaporizer ensured that all the fluid was in the gaseous phase and at a temperature at which fluid properties are well known. The discharge coefficient was determined with water for a range of Reynolds numbers. The orifice pressure and pressure drop were measured with strain-gage-type transducers and recorded on a self-balancing potentiometer. The flow-rate measurements are estimated to have an accuracy of  $\pm 2$  percent.

## PROCEDURE

### Establishment of Test Conditions

Obtaining information on boiling heat transfer for various heating rates at several pressure levels and over a range of flow rates in a systematic way was desired in order that the effects of each variable could be determined. It was also desired to have the test liquid enter the test section slightly subcooled and to study heat transfer and two-phase flow in forced flow over as great a range of fluid quality as possible and to obtain a critical heat flux at arbitrary locations along the tube axis. (The critical heat flux is defined as the flux immediately before the transition from the high upstream heat-transfer coefficient to a lower value.) Completely systematic operation was not always possible because of limitations of the test equipment and of the boiling process itself. In addition, operation at a precise preselected condition was difficult to attain because of fluctuations of flow and pressure that occurred in the system.

The general operating procedure consisted of setting conditions of flow rate, pressure, and inlet subcooling without heat addition and then gradually increasing the heat to the test section in small increments until the desired condition was obtained. As heat was added to the system, the flow and pressure conditions changed and had to be continually readjusted. The most consistent and repeatable results were obtained by always increasing the heat control setting and/or decreasing the flow rate. The range of test variables for the investigation of boiling heat transfer were test-section pressure, 30 to 74 pounds per square inch absolute; mass velocity, 2850 to 17,000 pounds per hour per square foot for hydrogen and 15,000 to 56,000 pounds per hour per square foot for nitrogen; inlet subcooling of  $0^{\circ}$  to  $9^{\circ}$  R for hydrogen and  $1^{\circ}$  to  $6^{\circ}$  R for nitrogen. The heated-tube-wall temperatures varied from  $36^{\circ}$  to  $1800^{\circ}$  R. The point of transition from a high to a lower heat-transfer coefficient was obtained at various locations along the length of the tube. Occasional unheated runs were made before and after a heated run. For an unheated run made after a heated condition, the flow and pressure controls were left unchanged in order that the effect of boiling on the flow conditions might be studied. A few runs were made in which cool hydrogen gas flowed through the tube at nominal pressures of 50 and 70 pounds per square inch absolute, inlet temperatures of  $46^{\circ}$

to 82° R, and mass velocities of 7800 to 13,000 pounds per hour per square foot.

### Data Reduction and Computations

All wall temperatures were obtained from the thermocouple chart readings and the aforementioned copper-constantan thermocouple calibration. Inner-tube-wall temperatures for a negligible axial temperature gradient were obtained from the calculations of appendix A. All pressures were read directly from the recorder charts. The flow rate was computed by the standard ASME orifice equations. Fluid properties were taken primarily from National Bureau of Standards sources (refs. 9 and 10).

The local heat flux was computed from the measured current and tube-outer-wall temperature by equation (All).

The local vapor quality was obtained from a heat balance by the relation

$$x = \frac{Q - wc_p(t_{\text{sat}} - t_{\text{in}})}{wh_{\text{fg}}} \quad (1)$$

(All symbols are defined in appendix B.) For the special case of negligible axial temperature gradient (hence, constant heat flux), the quality is given by

$$x = \frac{4 \left( \frac{q}{G} \right) \left( \frac{L}{D} \right) - c_p(t_{\text{sat}} - t_{\text{in}})}{h_{\text{fg}}} \quad (2)$$

Heat balances were computed for a few cases by comparing the enthalpy rise of the fluid through the test section with the amount of electric heat supplied to the test section. The heat balance could be computed only for cases with subcooled inlet liquid and superheated exit vapor (except for the hydrogen-gas runs) because there was no independent means of measuring quality. The heat balances agreed in most cases within ±10 percent. Usually the heat input was greater than the measured increase in fluid enthalpy, which indicated a heat loss. The main sources of heat loss (or gain) are the vacuum jacket, the copper ground bus, and the inlet and the exit sections. Calculations indicated that heat transfer across the vacuum jacket to the test section was negligible. Conduction through the copper ground bus was into the inlet section and was less than 5 percent of the heat generated in the tube. The heat loss from the tube through the walls of the inlet section was less than 2 percent of the heat generated in the tube. Evaluation of the heat loss at the exit of the test section was impossible. An additional source of error arose from the possible nonequilibrium of temperature and the phase of the test

fluid at the points of measurement in the inlet and the exit sections. The heat balance, however, was satisfactory and within the accuracy expected from the individual measurements.

## RESULTS AND DISCUSSION

### Tabulation of Data

The data obtained in 160 separate runs are tabulated in table II. Included in the table are data for runs both with liquid hydrogen and with liquid nitrogen, both heated and unheated, and also heated and unheated gaseous-hydrogen runs. The original data consisted primarily of the tube-outer-wall temperatures and the fluid exit bulk temperature obtained for various tests conditions of pressure, inlet fluid temperature, flow rate, and heating rate. For cases in which significant fluctuations of tube-wall temperatures occurred, the magnitudes of such fluctuations are also tabulated. The runs are numbered in chronological order. An omission in the run-number sequence indicates an aborted run or a significant change in the testing program. Also presented in table II are the temperatures measured on the electrical ground bus and in the inlet and the outlet sections. The table also contains the calculated values of the fluid inlet subcooling, the fluid exit superheat, the critical heat flux (or the uniform flux on the tube if it is below the critical value), the position of the point of transition in heat transfer (termed the critical-boiling-length-to-diameter ratio), and the local quality at the point of transition (termed the critical quality). The remarks tabulated for each run are based on observations made during the test and also on subsequent study of the data.

### Tube-Wall Axial-Temperature Profiles

The tube-outer-wall temperature profiles along the length of the tube for liquid-hydrogen tests at a pressure of approximately 50 pounds per square inch absolute and an average inlet subcooling of  $2^{\circ}\text{R}$  are presented in figure 3 for various heating rates at two different nominal mass velocities. Also included in the figure are the temperatures of the inlet and the outlet sections and a schematic diagram of the test-section geometry, including thermocouple locations. All the profiles of figure 3 have the same general shape but show trends with respect to heating rate and mass velocity. Starting at the tube inlet, the wall temperatures are essentially constant until a sudden temperature rise is obtained at various downstream locations. Following the initial sharp rise, the slope of the temperature profile decreases and in some cases the curves appear to approach a constant temperature. Listed in figure 3 are the values of the local heat flux existing immediately upstream of the

point of temperature rise. This heat flux, arbitrarily termed the critical heat flux, is indicative of a boiling heat-transfer condition at which, for a given flow and pressure, a transition occurs from a relatively large heat-transfer coefficient to a smaller coefficient at a specified position along the tube axis. (The flux downstream of the transition point is larger than the critical flux because of the increase in tube electrical resistance, but the proportionate increase in flux is much less than the increase in wall temperature.) The critical flux may not correspond to the maximum nucleate or burnout flux obtained in pool boiling; for the terms to be synonymous, evidence would be required that the critical heat flux results from surface ebullition.

All the data of figure 3 show an increase in the critical heat flux as the location of transition moves upstream. This inverse relation was also found in tests with water for transition occurring at the exits of tubes of various lengths (ref. 4). The temperature-rise curves for the nominal mass velocity of 12,000 pounds per hour per square foot (fig. 3(a)) show a more pronounced change in slope and tend to approach a constant value of temperature sooner than those for the lower flow rate (fig. 3(b)). These effects are probably related to the lower qualities at the critical point obtained at the higher flow rate; however, a difference in the two-phase flow pattern (void-fraction distribution) is felt to be the controlling factor.

All the wall temperatures of figure 3 upstream of transition are uniform along the tube within the limits of the instrumentation and show a small and nonsystematic variation between runs. The inner-wall temperatures can be obtained by subtracting the wall-temperature drop (given in appendix A) from the outer-wall temperatures of figure 3. The inner-wall temperatures are approximately  $12^{\circ}$  and  $3^{\circ}$  R above the inlet fluid saturation temperature for the conditions of figures 3(a) and (b), respectively. These small temperature differences are not considered accurate enough for further analysis because of the inherent inaccuracy and lack of sensitivity of the temperature measurements at these low temperatures ( $40^{\circ}$  to  $70^{\circ}$  R).

Since the highest wall temperatures obtained with hydrogen never exceeded  $900^{\circ}$  R and in most cases were less than  $600^{\circ}$  R, safe operation over a considerable range of conditions in a region equivalent to film boiling with forced flow seemed possible. Similar magnitudes of wall temperature were obtained in reference 8.

The tube-wall temperature profiles obtained with liquid nitrogen as the test fluid were generally similar to the results with hydrogen. (All nitrogen data are given in table II(b).) The rise in wall temperature following transition was much steeper for nitrogen than for hydrogen and the high temperatures (up to  $1800^{\circ}$  R) obtained finally caused failure of the test apparatus. During operation with liquid nitrogen,

attempts to obtain transition upstream of the tube exit generally resulted in unstable conditions with extreme fluctuations of flow, pressure, and wall temperature.

A few tests were made in which cool hydrogen gas flowed through the heated tube. These tests were made to obtain tube-wall axial temperature profiles for conditions of gas convective heat transfer for comparison with the temperature profiles obtained with boiling heat transfer. The profiles shown in figure 4 are for turbulent convective heat transfer and are considerably different from those obtained with boiling heat transfer (fig. 3). For the convective heat transfer, the tube-wall rise always started close to the tube inlet and the wall-temperature rise was generally more gradual than for the boiling heat-transfer tests. The shape of the convective wall-temperature profiles results primarily from entrance effects and variations in the tube-wall- to fluid-bulk-temperature ratio. The shape of the wall-temperature profiles for the boiling case (fig. 3), however, reflects changes in phase and in the boiling heat-transfer mechanism.

Temperature profiles are presented in figure 5 for boiling hydrogen at two constant values of transition location for several values of mass velocity and critical heat flux. An increase in mass velocity tends to skew the temperature-rise curves by increasing the slope at first and then by decreasing it at downstream locations. This effect of mass velocity on the temperature-rise curves was previously shown by the data of figure 3.

#### Critical Heat Flux

The critical heat flux for the conditions of this investigation corresponds to the local heat flux just upstream of the location of a sudden rise in wall temperature. For the critical heat flux at the end of the tube, transition was defined as the point corresponding to the conditions existing just previous to the increase in flux that first caused the thermocouple located 1/2 inch from the tube exit to rise. The critical heat flux obtained for boiling liquid hydrogen at a pressure of approximately 50 pounds per square inch absolute is presented in figure 6 as a function of mass velocity for four nominal values of the critical-boiling-length-to-diameter ratio  $L/D$ . All these curves show a significant increase in the critical flux with increasing mass velocity, but the slope of the curves generally decreases with increasing mass velocity. Generally the critical flux increases as the  $L/D$  decreases for constant mass velocity. Similar relations were found for water in reference 4, in which transition occurred at the exit of tubes of various lengths and diameters. In the present investigation, the length variation was obtained by causing transition to occur at various locations along a tube of constant length and diameter. The data of figure 6 show

an increased scatter with reduction in the critical  $L/D$ . The points of greatest heat flux in figure 6(d) also had the greatest fluctuations of wall temperature, flow rate, and pressure but were essentially steady-state conditions. The points along the lower envelope of critical flux in figure 6(d) did not show any fluctuation. Some of these lower points were obtained by deliberately overheating and then decreasing power and/or by increasing the flow rate until a stable condition was obtained. The rest of the lower points were obtained by a similar, but uncontrolled, process that could occur independently following a perturbation and that would eventually result in a stable condition. The highest flux values obtained at a given operating condition are arbitrarily termed the maximum critical heat fluxes. Throughout the investigation the maximum critical heat fluxes were generally associated with fluctuations of wall temperature, flow rate, and pressure, while the lower values of critical flux normally occurred without fluctuations. The scatter of the critical-flux values increased as the transition point moved upstream for the entire investigation with both liquid hydrogen and liquid nitrogen. The temperature profiles presented in figures 3 and 5 are from tests in which the maximum critical flux was obtained.

The temperature profile for a maximum-critical-heat-flux case is compared with the temperature profile obtained at a lower value of critical flux in figure 7. All other conditions of flow rate, pressure, and inlet subcooling are essentially the same. The main difference in the two profiles is a higher temperature level for the maximum critical flux case, which reflects the increased heating rate. The lower critical flux was obtained by deliberately overheating and then by cooling.

Tube-wall-temperature profiles for tests with critical heat fluxes less than the maximum are presented in figure 8 for an essentially constant mass velocity and various transition locations. For transition occurring at a value of  $L/D$  of less than 8 (axial distance  $L$  of about 4), the profiles each have a definite peak and a minimum as contrasted with the profiles for larger values of  $L/D$  and the profiles of figures 3 and 5.

Some runs were made with the wall-temperature rise occurring at or near the tube inlet. The resulting profiles are shown in figure 9 for two pressures and various mass velocities. Many of these curves have peaks and minimum points and in this respect are similar both to the profiles of figure 8 for values of  $L/D$  of less than 8 and to the profiles reported in reference 8. The shape of the curves of reference 8 was explained on the basis of an inlet end effect, a two-phase annular-flow model with the associated momentum pressure drop along the tube, and the attainment of "dry-wall" or "vapor-binding" conditions. In the tests presented herein, no measurable pressure drop across the test section was obtained, but dry-wall conditions could be attained. The data of figure 9 do not seem to indicate any significant effect on the critical

heat flux of the increase in pressure from 50 to 70 pounds per square inch absolute. Whether the critical-heat-flux values for the data of figure 9 should be classified as maximum or submaximum values is not known. Additional data for small values of transition length are necessary to resolve this question.

The critical-heat-flux data for hydrogen that are considered to be maximums are shown in figure 10 in logarithmic coordinates as functions of mass velocity for several critical  $L/D$ 's. Lines of constant quality of 1.00 and 0.50 computed from a heat balance are also indicated in figure 10. The general trend of the data is similar to that obtained for the boiling of water at low pressure (ref. 4). The water data indicated a change of slope or a knee in the curve of flux against mass velocity with the knee at a quality of approximately 0.50. The hydrogen data, however, do not exhibit any marked change in slope, particularly in the region of a quality of 0.50. The hydrogen data are fairly limited compared with the water data of reference 4. The hydrogen data can be extrapolated to higher and lower qualities in a manner which would show that a knee occurs in the quality range of 0.60 to 0.70. These same data are cross plotted against the critical-length-to-diameter ratio in figure 11, which shows the inverse relation between the critical heat flux and the critical  $L/D$ . This effect is greatest for high qualities. Extrapolating the curves to small critical values of  $L/D$  would indicate a small effect of  $L/D$  on the maximum critical flux. This condition makes it difficult to determine if the data shown in figure 9 represent maximum-critical-flux values.

The variation of the critical heat flux with mass velocity for boiling liquid nitrogen is presented in figure 12. The results are given for transition at the end of the tube only ( $L/D = 29$ ). For smaller values of critical  $L/D$ , the critical heat fluxes that were obtained were less than those of figure 12 at corresponding operating conditions. For this reason, the critical fluxes obtained upstream in the tube with nitrogen are not regarded as maximum critical fluxes as defined herein. Attainment of such maximum critical fluxes at critical values of  $L/D$  of less than 29 would be difficult and would require an improved apparatus with respect to stability control and material temperature limits. The general trend of the data of figure 12 agrees with that for hydrogen at a similar critical value of  $L/D$  (fig. 10) but with the critical flux at a larger value of mass velocity at approximately the same quality. This result reflects the lower latent heat of vaporization of nitrogen compared with hydrogen.

The data of figure 12 are also plotted in figure 13 together with the critical-flux data obtained with critical values of  $L/D$  of less than 29. The dashed line in figure 13 represents a quality of 1.00 for  $L/D$  of 29. With the exception of one point, all the critical-flux data for the short  $L/D$  tests fall below that for  $L/D$  of 29. In addition,

the critical flux obtained upstream of the tube exit appears to be independent of the location of transition over a considerable range of  $L/D$ . The resemblance between figure 13 of this report and figure 4 of reference 4 should be noted. Figure 4 of the reference for water (ref. 4) showed that the presence of compressible volumes limited the stability of the system and caused low values of critical flux. A similar, though unknown, limitation of system stability apparently existed for the nitrogen tests with transition upstream of the tube exit.

#### Normalization of Critical-Heat-Flux Data

Previous investigators (refs. 2 to 4) have tried various means of correlating and normalizing critical-heat-flux results. These efforts have been primarily empirical approaches. In reference 4, a large amount of data was normalized for forced-flow boiling of low-pressure water by using parameters including tube diameter, tube length, and mass velocity. The maximum-critical-heat-flux data of the present investigation are presented in terms of the parameters of reference 4 in figure 14 and compared with the water data of reference 4. The cryogenic data appear to be successfully normalized into single curves for each fluid with an acceptable degree of scatter. The normalized curves for the three fluids have the same general trends and are separated in the order of their respective latent heats of vaporization. A similar normalization of the data is shown in figure 15 but with slightly different powers of the length and the diameter terms. The normalization of the data in figure 15 appears to be equally as good as that in figure 14. Selection of the correct correlating parameters seems difficult without a realistic model of the two-phase flow and heat transfer, particularly for the cases of qualities approaching 0 and 1.00.

Acceptance of the normalization of the critical-heat-flux data in the form of figures 14 and 15 would imply an effect of the critical boiling length on the critical heat flux in addition to that required by a heat balance. If the length term is assumed to have no other effect than that required by a heat balance, the critical-flux data should be normalized by a plot of the critical flux against the mass velocity divided by the critical-length-to-diameter ratio  $L/D$ ; that is, the critical heat flux is a unique function of the local critical quality for a given fluid. The hydrogen maximum-critical-heat-flux data is shown in this way in figure 16. The dashed line represents a quality of 1.00 for all length values. The scatter of the data in figure 16 is only slightly worse than in figures 14 and 15. The actual data scatter appears to be unsystematic with the possible exception of the smallest  $L/D$  conditions, for which the heat-flux values fall lower than the rest of the data. Similar trends were obtained with the water data of reference 4; that is, the fluxes for small  $L/D$  data were low. The failure of the small  $L/D$  data to correlate with the rest of the results in a graph such as



figure 16 may be attributed to several factors, in addition to questions concerning the validity of the choice of correlating parameters. These are: (1) The data at small critical values of  $L/D$  were the most difficult to obtain and had the greatest tendency towards instability; (2) at short lengths, heat transfer and two-phase flow equilibrium may not have been achieved; and (3) the data at small values of  $L/D$  may be reflecting entrance effects. The relation between the maximum critical heat flux and the critical length has therefore apparently not been completely determined. An additional complicating factor is involved in the selection of the correct critical length. The water tests of reference 4 had considerable inlet subcooling and would be expected to have an appreciable length of subcooled boiling, whereas, in the present investigation, the subcooling was negligible and bulk boiling occurred over nearly the entire length. Whether the effective length should be measured from the tube inlet or from the location at which the fluid bulk reaches the local saturation temperature is unknown. This problem is treated in reference 3 in a discussion of the use of quality as a correlating parameter for the critical heat flux.

#### Wall Superheat

A conventional method of presenting boiling heat-transfer data (especially for pool or pot boiling) is a graph of the heat flux against the wall superheat (wall temperature minus the fluid saturation temperature). Data for nitrogen are presented in this form in figure 17. These data include both the maximum-critical-heat-flux conditions and conditions below critical (no transition). Most of the data appear to fall on a single curve with no significant effect of mass velocity. Included in figure 17 are the predictions of reference 11 for nitrogen and of reference 5 for nitrogen and water. It is claimed in reference 5 that the method presented therein of predicting boiling heat fluxes applies to flowing systems as well as to nucleate pool boiling. The results shown in figure 17 should not be interpreted as supporting the analytical predictions or their application to flowing systems. The agreement may be fortuitous, especially because of the limited extent and accuracy of the nitrogen data. Similar graphs for the hydrogen data are not presented because of the poor sensitivity of the copper-constantan thermocouples at hydrogen temperatures. In fact, the sensitivity of the thermocouples for the nitrogen conditions is considered marginal. Analytical predictions indicate a wall superheat of  $1^{\circ}$  to  $3^{\circ}$  R for the range of the hydrogen test conditions. The experimental data show a wall superheat of the order of  $10^{\circ}$  R or greater. Attributing this lack of agreement entirely to limitations of the thermocouples appears difficult. The data of reference 7 for hydrogen do not fully correlate with the analytical predictions of references 5 and 11.

## SUMMARY OF RESULTS

The results of the investigation of boiling heat transfer to liquid hydrogen and nitrogen in forced flow may be summarized as follows:

1. Boiling heat-transfer data (wall temperatures and heat fluxes) were obtained for bulk boiling of liquid hydrogen and nitrogen under forced flow upward inside an electrically heated tube. Data were obtained over ranges of flow and heating rates and pressures for small amounts of inlet subcooling. A limited amount of data was obtained with flowing cool hydrogen gas.
2. A transition in the type of boiling heat transfer was obtained. The critical heat flux corresponding to this transition was determined over a range of flow and heating rates and qualities. At specific combinations of flow and transition location, a range of critical-flux values was obtained and maximum values were determined. The maximum critical boiling heat flux increased with increasing fluid-flow rate and decreased with increasing length of tube before transition. The variation of the maximum critical flux with flow rate and critical boiling length was similar to that previously obtained with water.
3. Tube-inner-wall temperatures upstream of transition were essentially uniform and were only slightly greater (less than  $20^{\circ}$  R) than the fluid saturation temperature. Wall temperatures downstream of transition were considerably greater and the wall-temperature profiles generally resembled those obtained in film-boiling studies. The form of the wall-temperature rise downstream of transition appeared to be strongly dependent on the fluid quality at the point of transition. Maximum wall temperatures of  $900^{\circ}$  and  $1800^{\circ}$  R were obtained with hydrogen and nitrogen, respectively.
4. Fluctuations of pressure, flow rate, and temperature occurred during some of the boiling tests. Under some conditions, maximum critical-heat-flux values were attained during stable operation with fluctuations. In other cases the fluctuations became uncontrolled, and restabilization of the test condition resulted in critical-flux values less than the maximum values.
5. No measurable pressure drop across the test section was obtained at any condition.

Lewis Research Center

National Aeronautics and Space Administration  
Cleveland, Ohio, May 29, 1962

## APPENDIX A

## COMPUTATIONS AND DATA REDUCTION

## Temperature Drop Across Tube Wall

An analysis of the thermal and electric flow in an electrically heated tube is given in references 12 and 13. The basic assumptions of this analysis are negligible radial-voltage gradient and negligible axial-temperature gradient. For the case of a perfectly insulated outer wall, in which the thermal and electrical conductivities of the wall are linear functions of temperature, the equation for the temperature drop across a tube wall may be written as

$$t_{w,o} - t_{w,i} = \frac{JI^2 r_o^2 R_o \left(\frac{R_{av}}{R_o}\right)^2}{k_o A_c^2} \frac{F}{1 + \sqrt{1 - AF}} \quad (A1)$$

where

$$F = \ln\left(\frac{1}{1 - S}\right) - \left(S - \frac{S^2}{2}\right) \quad (A2)$$

$$S = 1 - \frac{r_i}{r_o} \quad (A3)$$

$$\frac{R_{av}}{R_o} = \frac{S - \frac{S^2}{2}}{S - \frac{S^2}{2} + \frac{BS^3}{6}} \quad (A4)$$

$$A = \frac{JI^2 r_o^2 R_o \left(\frac{R_{av}}{R_o}\right)^2}{A_c} \frac{\alpha_o}{k_o} \quad (A5)$$

$$B = \frac{JI^2 r_o^2 R_o \left(\frac{R_{av}}{R_o}\right)^2}{A_c^2} \frac{\beta_o}{k_o} \quad (A6)$$

(All symbols are defined in appendix B.) For the conditions of this investigation,

$$\left(\frac{R_{av}}{R_o}\right)^2 \approx 1$$

Substituting the proper constants and dimensions in equation (A1) gives the tube-wall-temperature drop as

$$t_{w,o} - t_{w,i} = 2465I^2 \frac{R_o}{k_o} \left( \frac{0.0131}{1 + \sqrt{1 - 0.0131 A}} \right) \quad (A7)$$

and

$$A = 2465I^2 \frac{R_o \alpha_o}{k_o} \quad (A8)$$

( $R_o = (\text{ohms})(\text{sq ft})/\text{ft}$ ;  $k_o = \text{lb force}/(\text{sec})(^\circ\text{R})$ ). The heat flux at the tube inner wall is given by

$$q = \frac{JI^2 R_o}{2\pi r_i A_c} \left( \frac{R_{av}}{R_o} \right) \quad (A9)$$

which for this investigation becomes

$$q = 5.22 \times 10^4 R_o I^2 \quad (A10)$$

( $R_o = (\text{ohms})(\text{sq ft})/\text{ft}$ ).

The variation of the thermal conductivity of 303, 304, and 347 stainless steel with temperature is given in figure 18. The variation of the tube electrical resistance with temperature is given in figure 19. The computed tube-wall-temperature drop is given in figure 20 as a function of the heat flux and the tube-outer-wall temperature. For the conditions of the investigation, the wall-temperature drop ranges up to  $20^\circ\text{R}$  for the hydrogen conditions and up to  $7^\circ\text{R}$  for the nitrogen test conditions. These computed wall-temperature drops should be applied only for readings of thermocouples located in a region of negligible axial-temperature gradient.

## Heat Flux

The local heat fluxes tabulated in table II were computed by

$$q = 282I^2R \quad (A11)$$

which is the same as equation (A10) with a change in the constant resulting from using the resistance in ohms per inch of tube. The heat fluxes tabulated in table II include not only the critical heat flux but also the heat flux at the end of the tube, which was essentially constant over the entire tube length for the subcritical flux conditions (no transition).

## APPENDIX B

## SYMBOLS

A	factor defined in eq. (A5), dimensionless
$A_c$	tube-wall cross-sectional area, $4.5 \times 10^{-4}$ sq ft
B	factor defined in eq. (A6), dimensionless
$c_p$	specific heat of liquid at constant pressure, Btu/(lb mass)(°R)
D	tube inside diameter, 0.04625 ft (0.555 in.)
F	factor defined in eq. (A2), dimensionless
G	test fluid mass velocity, lb mass/(hr)(sq ft)
$h_{fg}$	heat of vaporization, Btu/lb mass
I	heating current, amp
J	mechanical equivalent of heat, 778.3 ft-lb/Btu or 0.7376 lb force/(w)(sec)
k	thermal conductivity, Btu/(hr)(sq ft)(°R/ft) or lb force/(sec)(°R)
L	distance along tube axis measured from inlet station, in. (total length of tube, $16\frac{1}{8}$ in.)
p	pressure, lb/sq in. abs
Q	rate of heat flow, Btu/hr
q	heat flux, Btu/(hr)(sq ft)
R	tube electrical resistance, (ohms)(sq ft)/ft or ohms/in. of tube
r	radius measured from tube centerline, ft
S	factor defined in eq. (A3), dimensionless
t	temperature, °R
w	fluid mass-flow rate, lb mass/hr
x	fluid quality or mass fraction of vapor defined in eq. (1), dimensionless

- $\alpha$  coefficient of thermal conductivity as function of temperature,  
 $1/^{\circ}\text{R}$
- $\beta$  coefficient of electrical resistivity as function of temperature,  
 $1/^{\circ}\text{R}$

Subscripts:

- av arithmetical average
- cr critical (conditions at point of sudden rise of tube-wall temperature)
- ex exit of tube
- i inside surface of tube
- in inlet of tube
- o outside surface of tube
- sat saturation condition
- w wall of tube

## REFERENCES

1. Zuber, Novak, and Fried, Erwin: Two-Phase Flow and Boiling Heat Transfer to Cryogenic Liquids. Paper 1709-61, Am. Rocket Soc., Inc., 1961.
2. DeBortoli, R. A., et al.: Forced-Convection Heat Transfer Burnout Studies for Water in Rectangular Channels and Round Tubes at Pressure Above 500 Psia. WAPD-188, Westinghouse Electric Corp., Oct. 1958.
3. Silvestri, Mario: Two-Phase (Steam and Water) Flow and Heat Transfer. Paper 39, 1961 Int. Heat Transfer Conf., Boulder (Colo.), Aug. 28-Sept. 1, 1961.
4. Lowdermilk, Warren H., Lanzo, Chester D., and Siegel, Byron L.: Investigation of Boiling Burnout and Flow Stability for Water Flowing in Tubes. NACA TN 4382, 1958.
5. Forster, K. E., and Greif, R.: Heat Transfer to a Boiling Liquid - Mechanism and Correlations. Jour. Heat Transfer, ser. C, vol. 81, no. 1, Feb. 1959, pp. 43-53.
6. Aladyev, I. T., et al.: Boiling Crisis in Tubes. Paper 28, 1961 Int. Heat Transfer Conf., Boulder (Colo.), Aug. 28-Sept. 1, 1961.
7. Wright, C. C., and Walters, H. H.: Single Tube Heat Transfer Tests, Gaseous and Liquid Hydrogen. TR 59-423, WADC, Aug. 1959.
8. Hendricks, R. C., Graham, R. W., Hsu, Y. Y., and Friedman, R.: Experimental Heat Transfer and Pressure Drop of Liquid Hydrogen Flowing Through a Heated Tube. NASA TN D-765, 1961.
9. Scott, Russell B.: Cryogenic Engineering. D. Van Nostrand Co., Inc., 1959.
10. Johnson, Victor J.: A Compendium of the Properties of Materials at Low Temperature (Phase 1). Pt. 1. Properties of Fluids. TR 60-56, WADD, July 1960.
11. Chang, Yan-Po, and Snyder, Nathan W.: Heat Transfer in Saturated Boiling. Preprint 104, ASME-AIChE, 1959.
12. Powell, Walter B.: Heat Transfer to Fluids in the Region of the Critical Temperature. Prog. Rep. 20-285, Jet Prop. Lab., C.I.T., Apr. 1, 1956.



13. Kreith, F., and Summerfield, M.: Investigation of Heat Transfer at High Heat-Flux Densities: Experimental Study with Water of Friction Drop and Forced Convection with and without Surface Boiling in Tubes. Prog. Rep. 4-68, Jet Prop. Lab., C.I.T., Apr. 2, 1948.
14. Zimmerman, James E.: Heat Conduction in Alloys and Semi-Conductors at Low Temperatures. D.Sc. Thesis, Carnegie Inst. Tech., 1951.



TABLE I. - THERMOCOUPLE LOCATIONS

Description	Sta- tion	Distance from inlet (measured positively downstream), in., for -	
		Runs 100 to 220	Runs 220 to 327
Tube outer wall	1	0.5	0.52
	2	1.5	1.5
	3	2.5	2.5
	4	3.5	3.41
	5	4.5	4.5
	6	5.5	5.41
	7	6.5	6.45
	8	7.5	7.53
	9	8.5	8.53
	10	9.5	9.53
	11	10.5	10.5
	12	11.5	11.48
	13	----	14.06
	14	----	14.56
	15	15.6	15.61
Copper bus			
Far	16	$-1\frac{7}{8}$	-1.81
Near	17	$-7/8$	-.88
Inlet section			
Near	18	$-1/2$	-0.5
Far	19	$-1\frac{1}{2}$	-1.44
Outlet section	20	17	17.22

TABLE II. -

## (a) Hydrogen

Run	Pressure, lb sq in. abs	Satura- tion temper- ature, °R	Fluid- inlet temper- ature, °R	Fluid- exit temper- ature, °R	Inlet sub- cool- ing, °R	Exit super- heat, °ex - °sat, °R	Mass veloc- ity, lb mass (hr)(sq ft)	Heater current, amp	Critical heat flux, Btu (hr)(sq ft)	Critical- boiling- length- to- diameter ratio	Critical quality	Tube-outer-wall					
												1	2	3	4	5	6
100	47.8	45.0	138.0	138.0	---	93.0	6,480	---	---	---	---	157	151	148	145	145	145
101	51.0	45.5	89.0	89.0	---	23.5	7,725	---	---	---	---	90	82	81	81	79	81
103	53.0	45.9	82.0	117.0	---	71.1	7,780	254	---	---	---	174	209	225	238	245	255
105	49.0	45.2	52.0	52.0	---	6.8	13,100	---	---	---	---	69	69	69	69	65	69
106	50.2	45.4	54.0	92.0	---	46.6	12,800	326	---	---	---	148	200	223	261	280	306
107	49.0	45.2	46.0	96.0	---	52.8	12,550	332	---	---	---	160	226	265	305	336	375
108	52.5	45.8	55.0	121.0	---	75.2	7,780	346	---	---	---	61	248	354	442	492	533
109	70.5	48.3	57.0	107.0	---	58.7	12,500	348	---	---	---	189	272	326	385	458	498
114	49.5	45.3	40.2	45.9	5.1	.6	6,000	323	9,400	16.5	0.52	56	56	56	54	54	56
115	52.9	45.8	41.7	46.1	4.1	.3	12,500	462	19,350	19.2	.62	60	60	60	58	58	58
117	50.6	45.5	45.9	64.0	---	18.5	7,850	409	15,100	14.7	.65	58	58	60	56	56	56
118	74.0	49.1	43.7	48.6	5.4	-.5	9,050	376	12,750	19.0	.55	56	60	56	56	54	56
123	51.0	45.5	43.7	169.0	1.8	123.5	4,340	391	13,800	4.5	.31	58	60	60	323	393	441
124	51.0	45.5	43.9	240.0	1.6	194.5	2,850	375	12,700	4.5	.44	63	63	70	350	410	365
125	78.0	49.5	44.7	223.0	4.8	173.5	3,090	377	12,800	3.0	.23	60	64	290	361	408	455
126	76.0	49.2	43.2	222.0	6.0	172.8	3,090	379	13,000	4.2	.32	60	64	170	331	375	422
127	50.0	41.3	39.6	218.0	1.7	176.7	2,970	369	12,250	3.0	.25	56	60	316	437	486	533
128	50.0	45.4	44.2	45.5	1.2	.1	7,725	399	14,300	6.5	.26	58	60	60	60	60	60
129	50.3	45.4	43.9	45.3	1.5	-.1	12,800	417	15,700	11.7	.30	58	60	58	58	58	58
130	48.5	45.1	42.3	45.7	2.8	.6	7,500	412	15,300	15.7	.69	58	60	60	60	60	60
131	50.0	45.4	44.1	45.4	1.3	---	13,400	408	15,000	10.5	.25	60	60	60	60	60	60
132	50.0	45.4	44.1	45.7	1.3	.3	7,970	378	12,900	21.0	.76	60	60	60	60	60	60
133	48.0	45.0	44.4	70.0	1.6	25.0	5,530	360	11,700	17.0	.82	56	58	58	58	56	58
134	50.0	45.4	44.3	45.5	1.1	.1	5,650	339	10,400	20.0	.83	56	58	58	58	58	58
135	50.0	45.4	44.1	103.0	1.3	57.6	5,700	368	13,600	10.3	.55	58	58	58	58	58	58
136	50.0	45.4	44.3	45.3	1.1	-.1	5,830	359	11,800	15.5	.59	58	58	58	58	58	58
137	50.0	45.4	44.3	99.0	1.1	3.6	4,040	338	10,300	12.0	.69	56	56	56	56	56	56
138	50.0	45.4	44.4	149.0	1.0	103.6	4,040	371	12,400	8.5	.58	56	56	56	56	56	315
139	50.0	45.4	44.1	70.0	1.3	24.6	4,220	303	8,300	17.5	.77	56	56	56	56	56	56
140	50.0	45.4	44.2	83.0	1.2	37.6	4,100	320	9,300	15.8	.81	54	54	54	54	54	54
144	15.0	36.6	36.8	36.8	---	.2	---	---	---	---	---	45	47	47	47	45	47
145	69.0	48.3	46.5	46.7	1.8	-1.6	---	---	---	---	---	54	56	56	56	56	56
146	51.0	45.5	43.3	50.6	2.2	5.1	10,900	455	18,700	---	---	284	484	512	504	484	476
147	73.0	48.8	46.7	88.0	2.1	39.2	12,800	498	22,400	---	---	227	368	456	494	488	485
148	73.0	48.8	46.5	150.0	2.3	81.2	9,690	488	21,400	---	---	266	465	518	525	513	513
149	71.0	48.6	47.7	90.0	.9	41.4	10,600	527	25,100	---	---	250	422	514	539	519	512
150	71.0	48.6	48.0	88.0	.2	39.4	10,750	519	24,300	---	---	241	361	464	500	493	386
158	51.0	45.5	42.4	140.0	3.1	94.5	8,090	484	21,100	---	---	332	577	605	598	579	573
159	52.0	45.7	42.9	67.0	---	21.3	13,100	495	22,100	---	---	242	464	537	536	505	468
160	54.0	46.0	45.4	166.0	2.6	120.0	5,230	419	15,800	---	---	200	414	453	473	482	504
161	51.0	45.5	39.3	153.0	6.2	107.5	6,420	442	17,600	---	---	351	587	625	625	608	603
162	30.0	41.3	39.0	41.5	2.3	.2	13,500	463	19,300	---	---	356	605	598	546	500	472
163	31.0	41.5	39.1	90.4	2.4	48.9	13,500	523	24,600	---	---	492	826	771	664	589	580
164	52.0	45.7	42.7	168.0	3.0	122.3	6,060	448	18,100	---	---	267	490	531	545	549	562
165	52.0	45.7	42.8	132.0	2.9	86.3	6,680	483	21,000	---	---	303	575	604	591	567	560
166	50.0	45.4	39.1	137.0	6.3	91.6	8,390	463	21,000	---	---	260	537	597	597	574	572
167	52.0	45.7	39.0	166.0	6.7	120.3	5,770	447	18,100	---	---	192	446	503	525	530	545
168	71.0	48.4	39.0	178.0	9.4	129.6	7,380	512	23,700	---	---	171	453	570	599	593	604
169	71.0	48.4	39.0	150.0	9.4	101.6	8,150	508	23,300	---	---	182	447	542	568	560	561
170	69.0	48.3	44.1	74.2	4.2	25.9	15,200	513	23,700	---	---	122	381	490	537	518	505
171	65.0	47.7	45.4	158.0	2.3	110.3	7,020	468	18,700	---	---	199	497	536	543	539	547
172	70.0	48.4	46.0	141.0	2.4	92.6	8,440	490	21,700	---	---	260	534	570	564	548	552
202	49.8	45.4	43.2	43.0	2.2	-2.4	13,600	---	---	---	---	43	45	45	45	45	45
203	49.0	45.3	45.0	45.0	.3	-.3	13,875	363	11,900	a <sup>29+</sup>	a <sup>5</sup>	47	50	42	39	36	39
204	51.0	45.6	45.6	45.0	0	-.6	14,000	473	20,200	20.2	.67	60	59	54	50	45	42
205	50.1	45.4	41.4	44.9	4	-.5	12,900	457	18,850	19.5	.59	59	56	54	48	45	40
206	50.0	45.4	45.4	44.8	0	-.7	11,325	390	13,750	20.2	.57	52	54	50	50	45	45
208	49.0	45.3	42.4	44.7	2.9	-.6	9,535	458	19,000	8.0	.32	50	54	52	54	74	368
209	49.5	45.3	42.7	44.8	2.6	-.5	10,830	477	20,600	8.0	.31	50	54	54	56	70	368
210	48.5	45.1	42.4	44.8	2.7	-.3	11,690	518	24,350	8.5	.36	52	58	58	58	58	405
211	48.0	45.1	42.6	44.9	2.5	-.2	8,350	467	19,750	8.7	.43	52	54	54	54	54	329
212	49.2	45.3	43.5	43.5	1.8	-1.8	9,940	---	---	---	---	44	45	45	45	44	44
213	51.1	45.6	43.7	43.7	1.9	-1.9	12,525	---	---	---	---	43	45	45	45	44	45
214	50.2	45.4	42.9	44.8	2.5	-.6	9,240	200	13,560	a <sup>29+</sup>	a <sup>21</sup>	48	50	50	50	50	50
215	49.0	45.3	42.1	44.6	3.2	---	11,180	300	a <sup>8,150</sup>	a <sup>29+</sup>	a <sup>43</sup>	50	52	52	52	52	54
216	50.5	45.5	---	---	---	---	7,815	448	18,200	8.0	---	50	56	54	58	216	382
217	52.7	45.9	44.3	45.3	1.6	-.6	10,450	448	19,250	14.0	.54	54	60	60	62	62	65
218	52.8	45.9	44.3	45.5	1.6	-.4	13,235	465	21,350	14.0	.50	58	66	65	66	66	70
237	50.2	45.4	42.8	44.9	2.6	-.5	11,430	397	14,400	26.2	.72	48	64	60	56	66	64
238	46.5	44.8	42.3	42.3	2.5	0	14,375	---	---	---	---	50	60	54	52	54	52
239	50.4	45.5	43.4	44.0	2.1	-1.5	11,500	3									

## EXPERIMENTAL DATA

## (a) Hydrogen

temperature, °R, at station -								Copper bus temperature, °R		Inlet plenum wall temperature, °R		Exit plenum wall temperature, °R	Amplitude of tube wall temperature fluctuations, °R		Remarks
7	8	9	10	11	12	13	14	Far	Near	Near	Far	°R	±°R	At station -	
145	145	145	145	145	147	---	---	367	339	207	182	221	---	---	No-heat run
82	82	81	81	81	81	---	---	344	312	157	128	123	---	---	
263	271	275	283	288	291	---	---	345	310	158	131	162	---	---	
69	67	65	65	64	64	---	---	318	283	128	91	98	---	---	Cool-gas run
330	359	379	410	439	468	---	---	359	316	135	95	194	---	---	
420	469	510	554	590	609	---	---	379	335	139	102	211	---	---	Cool-gas run
560	577	585	595	598	599	---	---	377	330	109	59	233	---	---	
555	600	618	631	623	619	---	---	388	344	145	108	216	---	---	
58	58	58	160	279	319	---	---	356	305	87	49	99	---	---	Transition
60	60	58	60	60	244	---	---	411	352	92	49	185	---	---	
58	82	263	400	473	517	---	---	---	---	89	49	---	---	---	Transition; maximum-critical-flux value
58	58	58	60	66	249	---	---	---	---	---	---	---	---	---	
479	518	541	569	593	611	---	---	394	332	95	56	297	---	---	Transition
521	576	615	659	697	729	---	---	388	338	96	58	365	---	---	
498	545	579	620	644	687	---	---	388	336	90	60	377	---	---	Transition; maximum-critical-flux value
463	518	553	593	638	645	---	---	---	---	---	---	---	---	---	
574	618	643	676	700	720	---	---	---	---	---	---	---	---	---	Transition
332	389	414	427	434	440	---	---	---	---	---	---	---	---	---	
64	277	312	332	347	359	---	---	---	---	---	---	---	---	---	Transition; maximum-critical-flux value
60	60	60	305	382	430	---	---	---	---	---	---	---	---	---	
271	318	327	343	351	359	---	---	---	---	---	---	---	---	---	Transition
60	60	60	60	60	66	---	---	---	---	---	---	---	---	---	
58	58	58	87	308	369	---	---	---	---	---	---	---	---	---	Transition; maximum-critical-flux value
58	58	58	58	58	241	---	---	---	---	---	---	---	---	---	
301	379	420	458	486	509	---	---	---	---	---	---	---	---	---	Transition
58	58	69	256	330	373	---	---	---	---	---	---	---	---	---	
56	273	338	393	434	463	---	---	---	---	---	---	---	---	---	Transition; maximum-critical-flux value
390	450	485	521	545	577	---	---	---	---	---	---	---	---	---	
56	56	56	56	239	294	---	---	---	---	---	---	---	---	---	Transition
54	54	54	243	324	366	---	---	---	---	---	---	---	---	---	
47	47	45	45	45	45	---	---	358	290	92	47	54	---	---	No-heat run
56	58	58	58	58	56	---	---	347	297	86	58	64	---	---	
471	473	469	473	468	472	---	---	448	385	104	58	193	---	---	Transition
479	488	489	500	500	509	---	---	411	352	111	56	220	---	---	
519	536	534	547	556	582	---	---	408	355	109	56	246	---	---	Transition; maximum-critical-flux value
498	---	---	---	---	---	---	---	---	---	---	---	---	---	---	
480	495	483	495	495	504	---	---	416	362	111	58	191	---	---	Transition
587	572	570	583	583	588	---	---	384	332	95	57	185	---	---	
476	476	471	476	472	476	---	---	402	346	95	57	211	---	---	Transition
520	540	553	570	586	600	---	---	387	336	98	57	260	---	---	
596	596	577	595	592	593	---	---	390	338	95	51	285	---	---	Transition at inlet; critical length indeterminate
456	447	442	442	435	437	---	---	398	344	94	53	218	---	---	
537	535	531	536	531	534	---	---	414	360	97	52	189	---	---	Transition
568	581	591	610	618	626	---	---	392	339	98	57	294	---	---	
559	561	559	567	566	573	---	---	400	346	100	55	283	---	---	Transition
567	570	569	577	576	582	---	---	500	347	95	52	274	---	---	
553	570	575	590	600	606	---	---	393	341	100	55	287	---	---	Transition
615	632	640	659	675	697	---	---	400	348	96	57	320	---	---	
568	579	586	604	614	629	---	---	394	344	90	55	254	---	---	Transition
495	493	495	503	504	509	---	---	391	339	94	58	176	---	---	
554	573	577	594	604	616	---	---	402	349	105	57	260	---	---	No-heat run
539	568	572	585	592	604	---	---	400	349	105	57	260	---	---	
45	45	47	47	45	45	---	---	280	328	74	47	52	---	---	No transition
39	29	33	29	25	29	---	---	319	369	91	45	18	6	15	
42	40	40	36	29	227	---	---	343	398	102	54	173	2	12	Transition
45	42	36	40	40	276	---	---	342	389	94	53	144	---	---	
48	45	36	36	52	201	---	---	323	371	101	52	126	17	11	Transition; critical flux less than maximum
408	433	447	463	469	476	---	---	341	395	85	42	243	2	15	
422	447	458	472	481	484	---	---	347	402	88	42	239	2	9	Transition; long period required for stabilization; transition point moved slowly upstream
467	496	508	527	534	541	---	---	353	409	91	45	233	2	12	
413	456	479	506	523	534	---	---	358	392	88	42	264	2	15	Transition; with increase of heat, temperature at station 5 did not rise but downstream temperatures increased
45	45	44	44	44	44	---	---	285	334	72	45	52	---	---	
47	47	45	45	45	45	---	---	284	333	72	47	52	---	---	Transition; similar to run 210. Maximum-critical-flux value
52	52	52	52	52	54	---	---	294	345	79	47	60	---	---	
56	58	56	58	56	62	---	---	307	359	83	48	65	---	---	No-heat run
423	443	453	469	481	488	---	---	338	390	100	45	267	2	15	
68	70	294	386	434	484	---	---	340	394	101	48	244	14	1	Transition; maximum-critical-flux value
72	60	561	431	465	489	---	---	355	409	112	50	235	1	15	
62	62	62	106	72	66	73	72	294	339	68	66	66	40	10	No-heat run
52	52	52	500	54	50	50	50	272	315	50	50	52	---	---	
64	62	62	181	72	66	68	70	294	339	68	66	102	17	10	Transition; maximum-critical-flux value
64	64	64	---	72	68	119	218	296	341	70	68	86	26	13	
64	64	64	---	74	68	218	274	296	341	70	68	103	11	4	No-heat run; control valves in same position as in run 241
50	50	50	485	54	50	50	50	268	312	50	50	52	---	---	
66	66	66	---	79	95	499	507	307	356	350	409	219	1	14	Transition; maximum-critical-flux value
52	52	52	459	54	52	50	50	268	311	50	50	52	---	---	
54	54	54	52	60	56	56	75	272	314	54	54	56	15	14	No-heat run; control valves in same position as in run 243
64	62	62	499	47	39	39	39	258	301	39	39	42	---	---	
50	50	50	83	56	52	56	54	269	314	52	52	52	30	13	Transition; maximum-critical-flux value
42	39	39	490	47	42	39	39	260	304	39	39	42	---	---	

TABLE II. - Concluded.

## (a) Concluded. Hydrogen

Run	Pressure, lb sq in. abs	Saturation temperature, °C	Fluid-inlet temperature, °C	Fluid-exit temperature, °C	Inlet sub-cooling, °C	Exit superheat, °C	Mass velocity, lb mass (hr)(sq ft)	Heater current, amp	Critical heat flux, (hr)(sq ft)	Critical-boiling length-to-diameter ratio	Critical quality	Tube-outer-wall					
												1	2	3	4	5	6
253	51.9	45.7	42.3	45.4	3.4	-0.2	4,520	263	6,250	25.7	0.77	39	73	50	50	54	52
254	51.0	45.6	42.4	45.4	3.2	-2	4,500	268	6,500	26.0	.82	42	77	50	29	54	52
255	49.8	45.4	42.4	45.1	3.0	-3	4,380	272	6,700	24.5	.81	42	77	50	42	54	52
256	51.0	45.6	43.1	45.3	2.5	-3	4,450	313	8,850	20.5	.90	42	80	52	45	58	54
257	46.0	44.7	43.5	44.3	1.2	-4	4,300	---	---	---	---	39	70	45	45	45	42
258	14.7	36.4	36.4	36.4	0	0	0	---	---	---	---	33	70	36	36	36	33
259	50.0	45.4	43.2	45.5	2.2	1	4,100	291	7,700	21.5	.89	45	82	54	45	58	54
260	49.5	45.3	42.5	45.7	2.8	-4	4,170	312	8,800	20.5	.95	36	74	50	45	54	52
261	50.0	45.4	42.4	42.8	3.0	-2.6	4,535	---	---	---	---	42	70	47	45	47	45
262	50.2	45.4	43.4	45.5	2.0	.1	4,030	316	9,050	19.0	.95	42	80	52	50	58	56
263	49.5	45.2	43.5	45.5	1.7	35.3	4,470	351	11,150	15.2	.85	45	86	54	66	60	58
297	47.0	44.9	43.5	44.6	1.4	-3	6,770	317	9,100	25.0	.75	50	86	58	58	62	58
298	47.7	45.0	43.6	44.9	1.4	-1	6,520	316	9,050	25.2	.78	50	88	58	68	64	60
299	48.4	45.1	43.7	45.0	1.4	-1	6,780	312	8,800	26.2	.76	50	88	58	58	62	60
300	46.1	44.7	43.7	44.8	1.0	.1	8,720	363	11,950	26.2	.81	50	90	58	---	66	62
301	52.3	45.8	43.0	45.5	2.8	-3	4,440	263	6,300	26.2	.82	48	80	54	47	60	56
302	52.0	45.7	43.1	45.6	2.6	-1	10,630	387	13,600	26.2	.73	48	85	60	59	68	64
303	50.5	45.5	43.1	45.4	2.4	-1	12,620	416	16,700	26.2	.71	48	86	60	52	68	64
304	50.4	45.5	43.4	45.4	2.1	-1	16,960	458	19,150	26.2	.65	48	86	64	50	74	70
305	50.0	45.4	43.6	---	1.8	---	7,990	433	17,150	12.0	.56	48	83	66	64	75	74
306	49.0	45.1	43.1	---	2.0	---	7,990	424	16,400	7.2	.30	70	79	72	72	385	443
307	49.8	45.4	43.6	45.4	1.8	0	5,740	373	12,600	16.2	.89	48	83	56	42	66	62
308	49.8	45.4	43.3	45.9	2.1	.5	5,510	382	13,200	15.7	.83	48	82	58	58	66	64
309	50.6	45.5	43.2	46.2	2.3	.7	6,050	389	13,750	14.0	.69	50	83	58	58	66	66
310	49.0	45.2	43.3	45.9	1.9	.7	8,330	440	17,650	13.5	.63	50	85	62	62	74	72
311	51.6	45.7	42.3	45.7	3.4	0	13,380	443	17,850	7.5	.17	45	79	62	54	269	390
312	53.0	45.9	44.9	46.0	1.0	.1	12,660	470	20,050	15.0	.53	47	93	62	---	74	72
313	50.9	45.6	41.2	45.5	4.4	-1	16,200	415	15,650	5.0	.04	45	75	60	327	389	393
314	50.5	45.5	41.7	45.5	3.8	0	16,000	424	16,300	10.0	.17	47	75	60	54	66	100
315	50.8	45.6	41.7	45.5	3.9	-1	16,680	425	16,350	12.5	.22	47	73	60	54	66	60
316	51.5	45.7	42.9	46.2	2.8	-.5	11,200	444	17,900	13.5	.45	47	88	58	58	66	60
317	52.1	45.8	43.5	45.4	2.5	108.2	5,820	378	12,950	8.7	.84	42	75	52	52	58	277
318	50.8	45.6	43.8	45.8	1.8	0	6,180	397	14,500	8.5	.42	42	77	52	52	58	261
319	51.8	45.7	43.6	46.0	2.1	.3	9,310	419	15,900	8.5	.30	39	75	52	45	62	298
320	51.8	45.7	44.6	45.8	1.1	.1	10,920	430	16,750	8.5	.25	39	80	62	36	64	276
321	49.8	45.2	44.6	45.4	.6	2	11,850	447	18,150	8.5	.29	36	79	54	47	70	292
322	51.5	45.7	45.6	---	.1	---	8,700	448	16,150	2.5	.12	45	97	268	505	374	459
323	50.0	45.4	45.5	45.5	-1	.1	10,890	---	---	---	---	45	80	50	47	47	45
324	52.2	45.6	44.2	45.7	1.6	-1	14,670	476	20,500	15.2	.46	42	75	58	52	66	64

## (b) Nitrogen

264	55.3	163.2	162.0	165.0	1.2	1.8	17,030	297	8,870	21.5	0.57	165	198	170	175	173	171
265	54.1	162.6	158.0	164.8	4.8	1.2	24,030	304	9,250	25.0	.46	163	195	169	171	172	171
266	54.6	163.0	160.0	165.0	3.0	2.0	24,300	322	10,420	23.7	.50	160	197	170	179	174	172
267	50.2	161.4	158.0	161.0	3.4	-4	38,000	345	11,800	25.0	.38	162	195	169	167	171	171
268	48.5	160.7	157.5	160.5	3.2	-2	30,400	323	10,400	23.5	.39	160	194	167	171	170	170
269	54.3	163.0	160.0	163.0	3.0	0	29,800	313	9,800	21.5	.35	165	197	170	174	173	172
270	56.0	163.5	161.5	163.5	2.0	0	42,300	355	12,600	24.2	.36	165	197	170	165	175	173
271	50.2	161.4	157.0	162.0	4.4	.6	31,000	325	10,600	24.0	.39	161	193	167	171	171	170
272	49.8	161.2	157.0	162.0	4.2	.8	30,800	326	10,850	24.9	.49	161	193	168	173	171	170
273	50.1	161.3	157.0	160.5	4.3	-.8	15,700	309	8,550	a29+	a.87	163	195	167	169	170	169
274	49.8	161.2	158.0	160.5	3.2	-7	15,100	314	a9,850	a29+	a.95	161	194	165	168	169	168
275	55.3	163.2	157.5	163.0	5.7	-2	19,750	301	9,050	22.0	.48	162	194	167	163	171	170
276	50.4	161.4	158.0	160.5	3.4	-.9	16,250	316	a10,000	a29+	a.89	163	195	167	165	171	170
277	52.5	162.2	159.0	162.0	3.2	-2	22,850	302	9,150	22.5	.44	164	198	169	167	172	171
278	52.0	162.0	159.0	162.0	3.0	0	27,200	316	10,000	24.0	.43	164	197	169	175	171	170
279	50.0	161.3	157.0	161.0	4.3	-.3	25,100	352	a12,350	a29+	a.70	159	194	165	171	170	169
280	50.0	161.3	157.0	162.0	4.3	.7	24,400	367	13,300	29.0	.78	159	194	165	176	170	169
281	50.5	161.4	157.0	161.0	4.4	-.4	24,100	361	a13,000	a29+	a.77	159	194	166	165	171	170
282	50.6	161.5	157.5	161.0	4.0	-.5	23,800	371	13,800	29.0	.84	160	195	166	165	171	170
283	50.3	161.4	158.0	162.0	3.4	.6	24,500	308	9,500	23.5	.44	160	191	165	167	168	167
284	51.0	161.7	158.5	161.5	4.8	1.2	31,500	400	a16,700	a29+	a.77	160	197	167	171	172	171
285	54.4	163.0	159.0	163.0	4.0	0	31,500	400	16,000	29.0	.73	160	198	168	171	173	172
286	55.0	163.2	159.0	163.0	4.2	-.2	31,700	408	16,500	29.0	.75	161	200	170	178	174	173
287	55.0	163.2	159.0	163.0	4.2	-.2	31,100	413	a17,100	a29+	a.79	160	200	170	166	173	172
288	50.2	161.4	157.0	160.0	4.4	-.4	41,900	453	a20,550	a29+	a.70	160	201	170	176	175	172
289	50.5	161.4	156.5	160.5	4.9	-.9	40,800	453	20,550	29.0	.72	161	202	170	168	174	173
291	49.2	160.8	157.0	161.0	3.8	.2	41,700	346	11,950	24.0	.40	160	194	167	171	171	170
292	50.6	161.5	158.0	161.0	3.5	-.5	56,300	489	a24,000	a29+	a.61	161	205	171	172	177	176
293	49.8	161.2	157.0	161.0	4.2	-.2	32,400	154	a2,350	a29+	a.08	159	197	162	167	163	162
294	49.5	161.1	157.0	161.0	4.1	-.1	31,400	208	a4,300	a29+	a.18	160	198	163	167	164	163
295	49.7	161.1	157.0	161.0	4.1	-.1	31,200	255	a5,500	a29+	a.28	160	199	163	169	167	164
296	49.6	161.1	157.0	161.0	4.1	-.1	31,700	323	a10,400	a29+	a.46	160	192	165	170	168	167
325	47.5	160.2	159.5	159.7	1.7	-.5	31,900	---	---	---	---	160	184	169	163	160	160
326	49.9	161.3	159.0	161.0	2.3	-.3	28,000	325	10,550	17.0	.31	161	197	166	166	171	167
327	51.3	161.8	159.7	162.0	2.1	.2	24,400	384	14,700	3.0	.08	164	294	833	1132	1320	1455
328a	50.0	161.2	158.2	---	---	---	30,800	410	17,000	28.0	.80	---	---	---	---	---	---
329a	50.0	161.2	158.2	---	---	---	37,500	469	21,300	29.0	.82	---	---	---	---	---	---
275a	50.4	161.4	158.0	161+	3.4	0	15,500	313	10,000	29.0	.93	---	---	---	---	---	---
292a	51.0	161.7	158.0	162.0	3.7	.3	53,600	503	25,800	29.0	.69	---	---	---	---	---	---
329a	50.5	161.5	158.5	161+	3.0	0	24,000	387	13,500	29.0	.82	---	---	---	---	---	---
329a	49.9	161.0	159.0	161.0	2.0	0	30,400	390	15,300	29.0	.73	---	---	---	---	---	---

## EXPERIMENTAL DATA

## (a) Concluded. Hydrogen

temperature, °R, at station -										Copper bus temperature, °R		Inlet plenum wall temperature, °R		Exit plenum wall temperature, °R		Amplitude of tube wall temperature fluctuations		Remarks
7	8	9	10	11	12	13	14	15		Far	Near	Near	Far			±°R	At station -	
50	50	50	94	58	52	85	100	171	272	316	52	52	54	30	13			Transition; maximum-critical-flux value
52	52	52	90	58	52	62	80	122	274	318	54	54	54	8	13			
52	52	52	80	58	52	52	108	119	274	318	54	52	56	20	14			
52	54	54	91	66	179	379	392	375	280	325	294	242	183	14	12			No-heat run; control valves in same position as in run 256 Vented system to atmosphere
42	42	42	504	47	42	39	39	42	263	307	42	42	45	---	---			
33	33	33	505	36	33	29	29	33	262	308	33	29	36	---	---			
56	54	54	90	64	58	328	341	329	281	326	249	192	145	2	14			Transition; maximum-critical-flux value
52	52	52	108	62	172	402	413	397	281	326	315	266	285	4	12			
45	45	45	---	50	45	42	42	42	268	311	45	45	45	---	---			
54	56	56	566	103	260	428	437	421	287	333	346	306	211	23	11			No-heat run; control valves in same position as in run 280 Transition; maximum-critical-flux value; difficult to stabilize because of flow oscillations
56	56	109	549	589	443	592	605	564	293	338	489	455	272	21	9			
58	56	56	60	68	60	124	235	188	287	332	62	60	60	49	13			
58	58	58	62	68	62	91	167	188	287	331	62	60	60	26	13			Transition; maximum-critical-flux value
58	58	58	62	70	62	62	66	155	287	332	62	60	60	12	14			
56	60	60	60	62	72	64	64	70	230	294	66	64	88	6	4			
56	54	54	56	64	58	80	83	105	283	327	60	58	60	17	14			Transition; maximum-critical-flux value
62	62	62	64	72	66	68	72	108	296	343	68	66	64	38	15			
64	62	64	66	72	68	70	72	236	301	347	70	68	105	5	15			
68	68	68	70	72	72	74	80	203	307	354	74	72	100	6	15			Transition; conditions impossible to stabilize; temperatures kept changing
75	361	423	461	492	509	568	571	538	303	350	529	519	270	---	---			
451	457	466	470	480	489	511	512	489	302	349	490	488	241	---	---			Transition; maximum-critical-flux value
60	60	60	62	280	344	511	522	486	296	343	439	401	243	---	---			
60	62	62	294	375	428	568	578	544	297	344	492	460	268	1	14			
64	64	305	375	420	451	524	554	521	298	346	491	467	266	---	---			Transition
72	132	387	439	471	492	556	564	535	307	354	525	514	269	---	---			
424	416	406	405	409	410	424	429	409	309	359	411	409	207	---	---			
68	68	239	375	413	434	504	511	487	314	361	465	450	231	---	---			Transition; maximum-critical-flux value
373	351	357	351	353	348	347	352	332	300	335	313	316	140	---	---			
365	380	375	372	370	366	362	368	349	301	347	358	359	148	---	---			
58	326	351	355	361	361	361	362	346	300	346	357	357	143	---	---			Transition; maximum-critical-flux value
56	104	352	387	411	426	469	472	450	302	349	445	439	222	---	---			
360	407	447	487	523	553	665	665	635	294	340	609	583	329	8	13			
359	398	415	430	451	463	517	520	493	285	342	487	476	260	---	---			Transition
377	392	404	409	418	421	444	447	424	289	346	427	425	212	---	---			
365	393	406	412	418	420	441	444	418	300	348	423	416	204	13	4			
392	422	434	433	441	442	459	463	436	303	350	431	430	187	---	---			Transition; took 3 hr to obtain equilibrium; at first had increasing temperature profile; later profile peaked
353	618	628	596	575	561	573	577	540	319	364	555	561	270	4	12			
45	45	45	45	50	45	42	42	45	276	321	47	47	45	---	---			
54	50	101	473	420	441	479	482	455	308	357	462	454	213	---	---			No-heat run to check wall thermocouples Transition; similar behavior as in run 322

## (b) Nitrogen

171	173	172	173	178	175	885	890	850	348	384	549	178	175	---	---			Transition; on all these runs either power was decreased or flow rate increased as desired transition condition was approached to prevent overheating and instability
171	172	171	172	175	173	451	618	524	348	380	175	174	174	3	15			
172	173	172	173	176	174	705	785	635	345	383	177	175	175	3	15			
171	172	171	171	174	172	552	725	629	345	383	173	173	173	2	15			No transition; close to maximum-critical-flux value
170	170	170	170	173	171	805	850	660	341	377	173	171	171	4	15			
172	174	173	175	178	176	805	830	626	340	376	---	179	175	---	---			
173	174	173	174	177	175	875	800	660	346	383	175	175	173	5	15			No transition
170	171	170	171	173	171	725	805	639	337	373	173	173	172	---	---			
170	171	170	171	173	171	173	173	172	336	371	172	172	171	---	---			
169	170	170	170	171	171	172	172	172	343	380	171	171	170	---	---			Transition; close to maximum-critical-flux value
168	169	168	168	170	169	171	170	170	343	380	170	170	168	---	---			
170	171	170	171	174	172	780	795	590	340	377	174	173	172	---	---			
170	170	170	170	172	171	173	173	172	345	382	171	171	170	---	---			No transition; close to maximum-critical-flux value
171	171	171	171	175	172	721	764	601	343	380	175	173	172	3	15			
170	171	170	171	173	172	660	781	619	346	383	174	173	172	2	15			
168	169	168	168	169	171	170	171	171	342	379	171	171	170	---	---			Transition
168	169	168	168	169	171	170	805	981	343	380	171	171	170	12	13			
169	170	169	169	171	170	172	172	172	346	381	171	171	170	11	14			
168	169	168	170	171	170	171	171	171	344	381	171	171	170	---	---			No transition
169	170	169	170	171	170	172	172	172	346	383	171	171	170	---	---			
167	168	167	168	170	169	860	735	598	337	373	170	170	169	1	15			
170	171	171	171	172	171	173	174	173	351	390	172	172	171	---	---			Transition; maximum-critical-flux value
171	172	171	172	175	173	175	176	174	350	380	173	173	172	---	---			
172	173	172	173	175	174	176	178	175	352	391	174	174	171	---	---			
171	172	172	173	174	173	175	176	174	353	392	174	174	171	3	4			No transition; close to maximum-critical-flux value
171	172	171	172	176	173	175	176	174	351	392	174	174	171	---	---			
172	173	172	173	176	174	175	177	175	362	404	174	174	171	---	---			
169	170	169	170	172	171	890	793	642	343	381	173	172	172	4	15			Transition
174	175	174	175	178	177	179	178	175	369	411	176	177	171	---	---			
163	163	163	163	164	163	164	164	165	325	361	163	163	166	---	---			
164	164	163	164	165	165	167	166	167	328	365	166	165	167	---	---			No transition
165	166	165	167	168	167	168	168	168	333	370	167	167	168	---	---			
167	168	167	169	170	169	171	171	170	342	380	170	170	170	---	---			
160	160	160	160	160	160	160	160	160	318	358	160	160	160	---	---			No-heat run; thermocouple check
168	169	168	388	776	900	1175	1170	890	348	385	1055	978	159	3	10			
1635	1585	1685	1730	1760	1785	1745	1770	1600	470	494	1801	1815	765	5	6			Transition; difficult to control
---	---	---	---	---	---	---	---	---	---	---	---	---	---	---	---			
---	---	---	---	---	---	---	---	---	---	---	---	---	---	---	---			
---	---	---	---	---	---	---	---	---	---	---	---	---	---	---	---			All these data taken while attempting to obtain maximum critical flux for transition at end of tube; data represent last readings taken before final power or flow adjustment, which caused instability and gave transition upstream at heat-flux values considered to be less than maximum critical flux
---	---	---	---	---	---	---	---	---	---	---	---	---	---	---	---			
---	---	---	---	---	---	---	---	---	---	---	---	---	---	---	---			

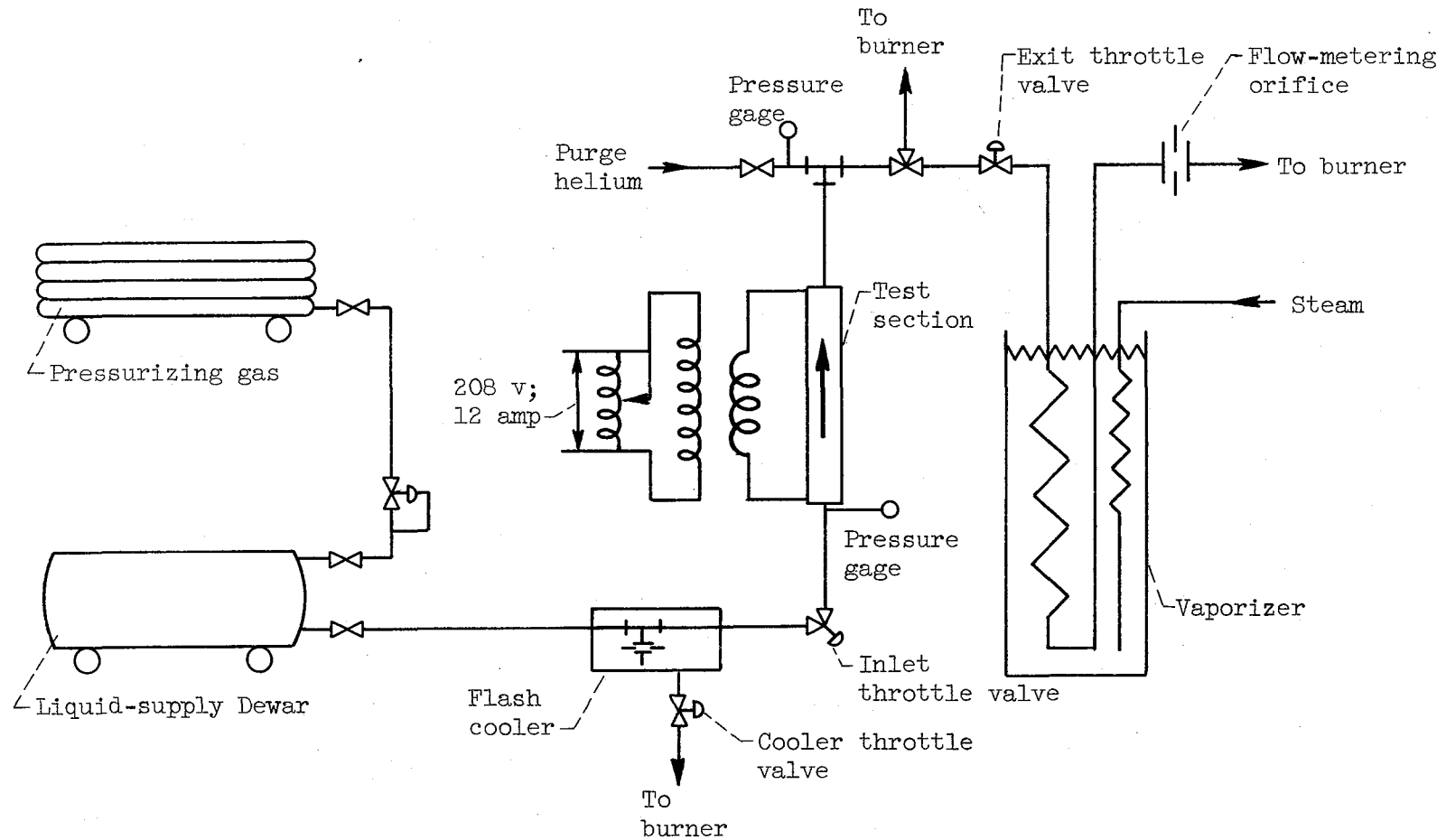


Figure 1. - Schematic drawing of cryogenic boiling-heat-transfer apparatus.



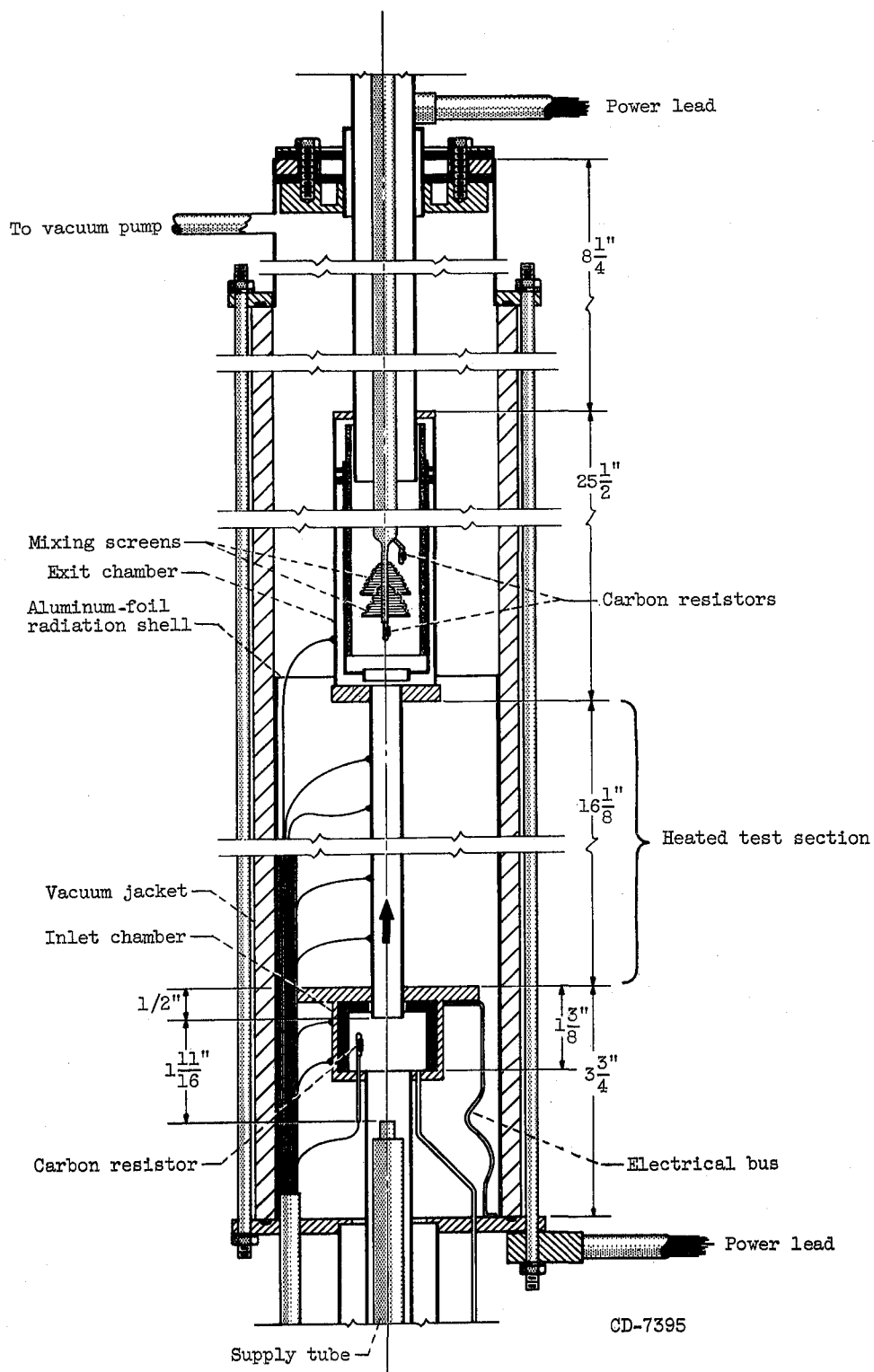
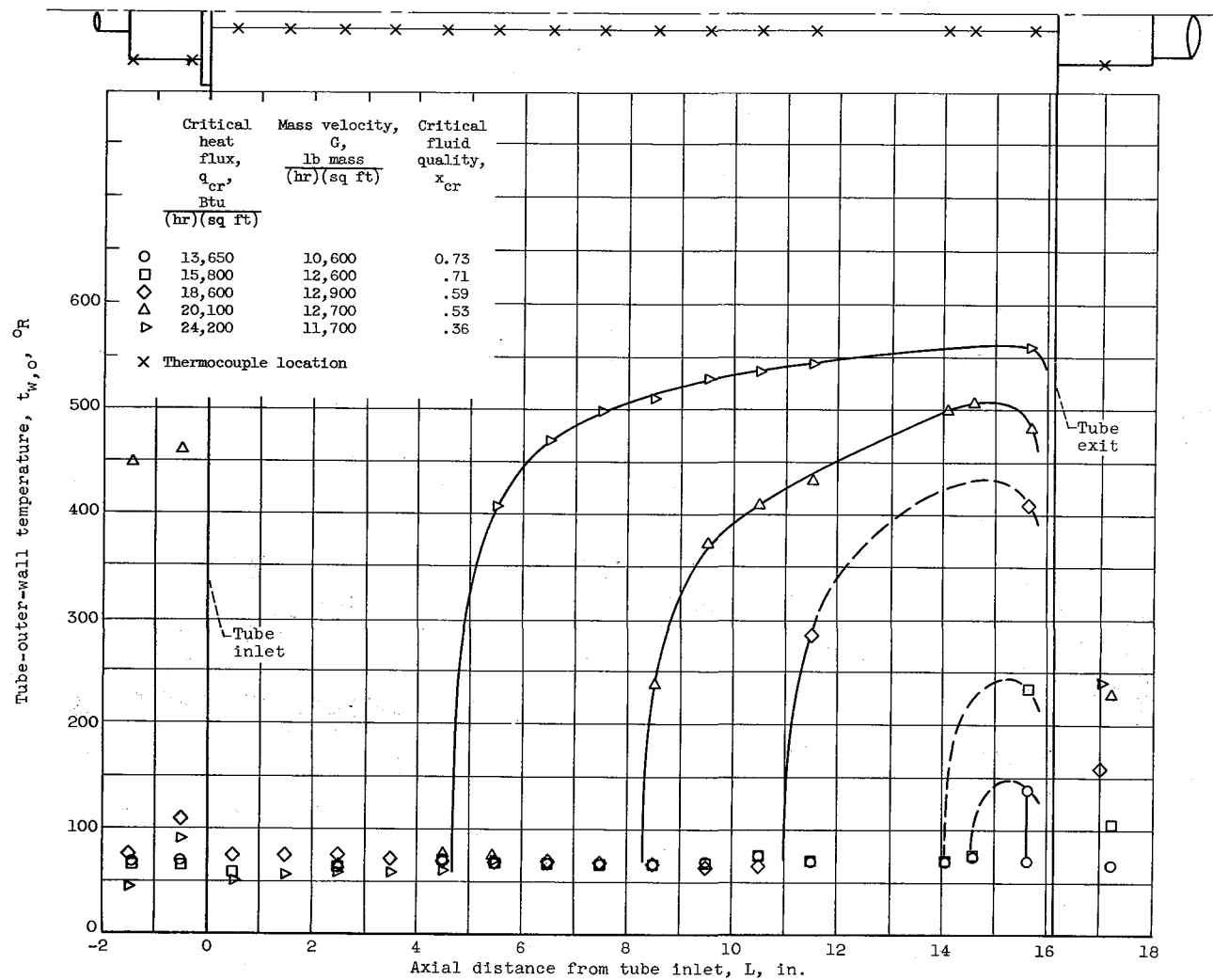
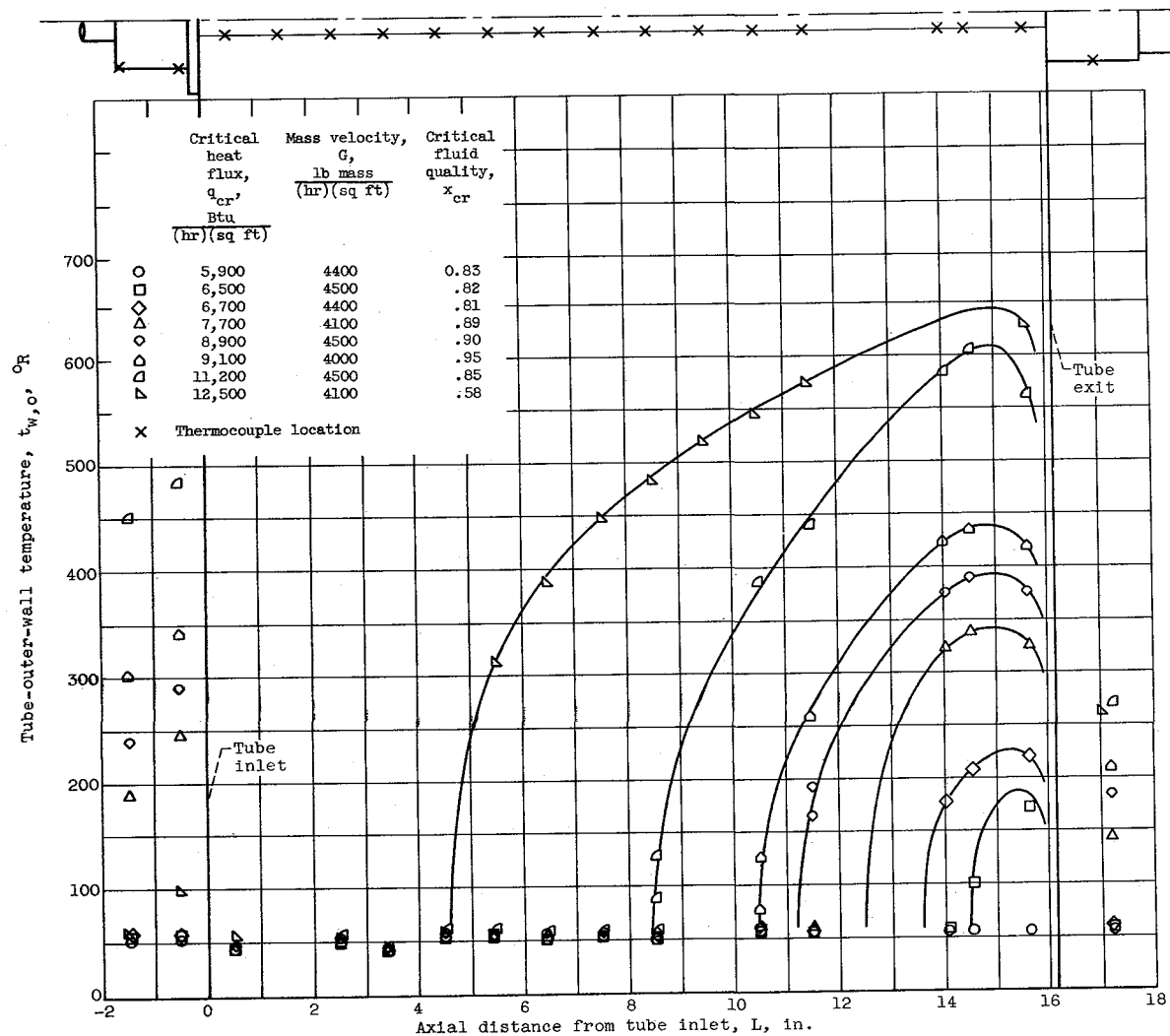


Figure 2. - Details of test section, inlet, and exit.



(a) Mass velocity, approximately 12,000 pounds per hour per square foot.

Figure 3. - Tube-outer-wall temperature profiles for constant mass velocity and varying heat flux and location of transition. Liquid hydrogen; test-section pressure, approximately 50 pounds per square inch absolute; average inlet subcooling, 2° R.



(b) Mass velocity, approximately 4500 pounds per hour per square foot.

Figure 3. - Concluded. Tube-outer-wall temperature profiles for constant mass velocity and varying heat flux and location of transition. Liquid hydrogen; test-section pressure, approximately 50 pounds per square inch absolute; average inlet subcooling, 2° R.

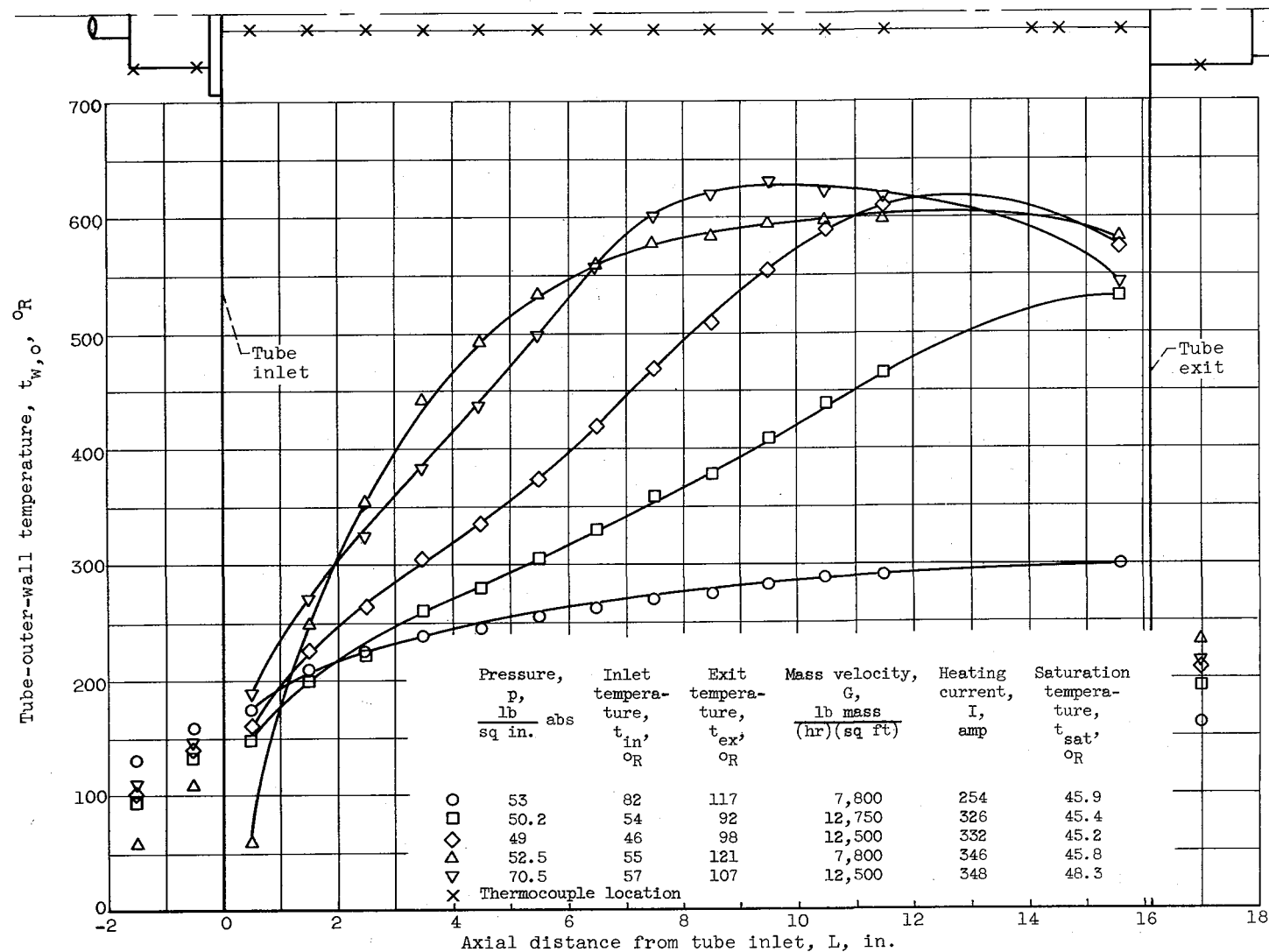
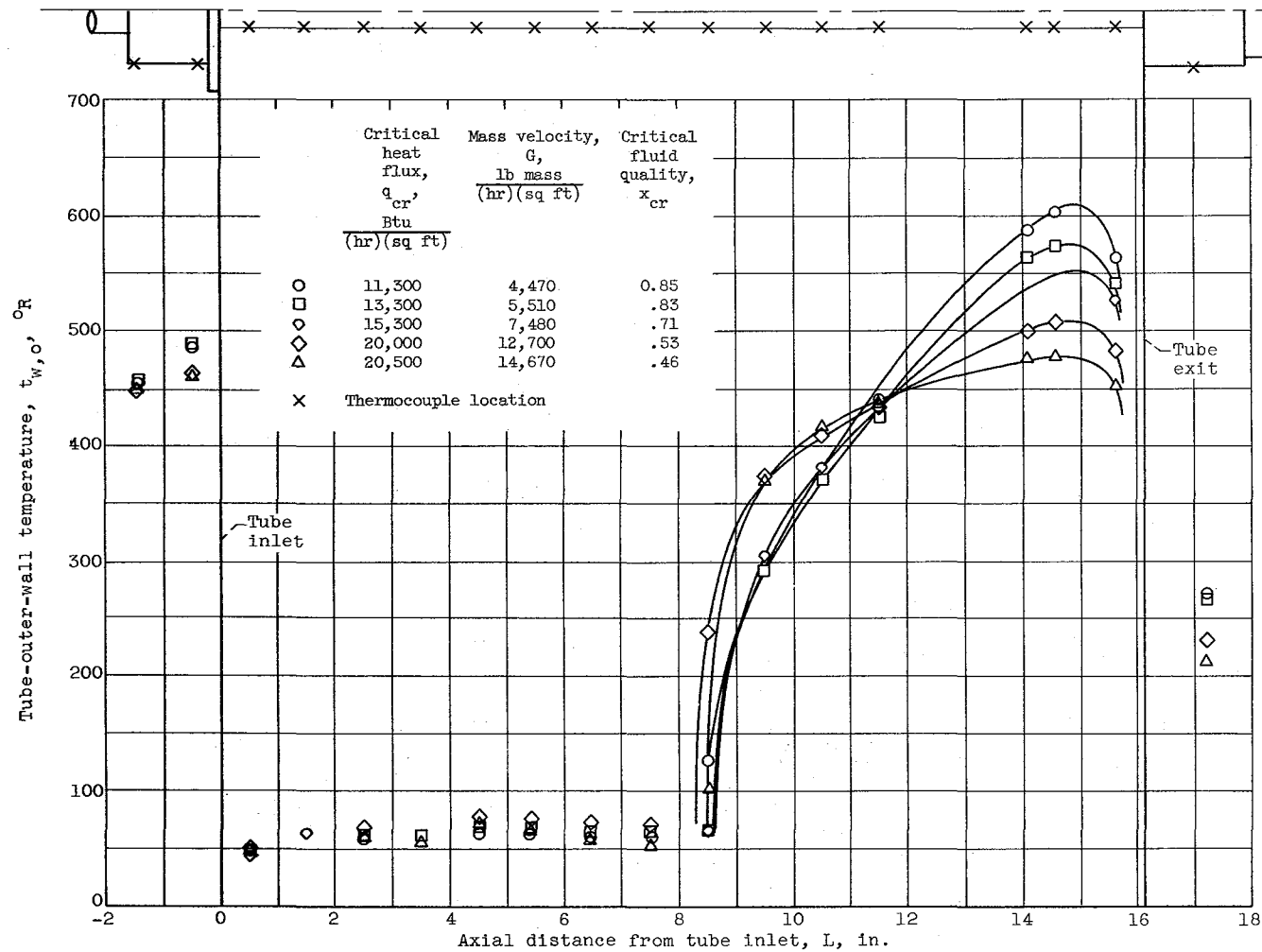
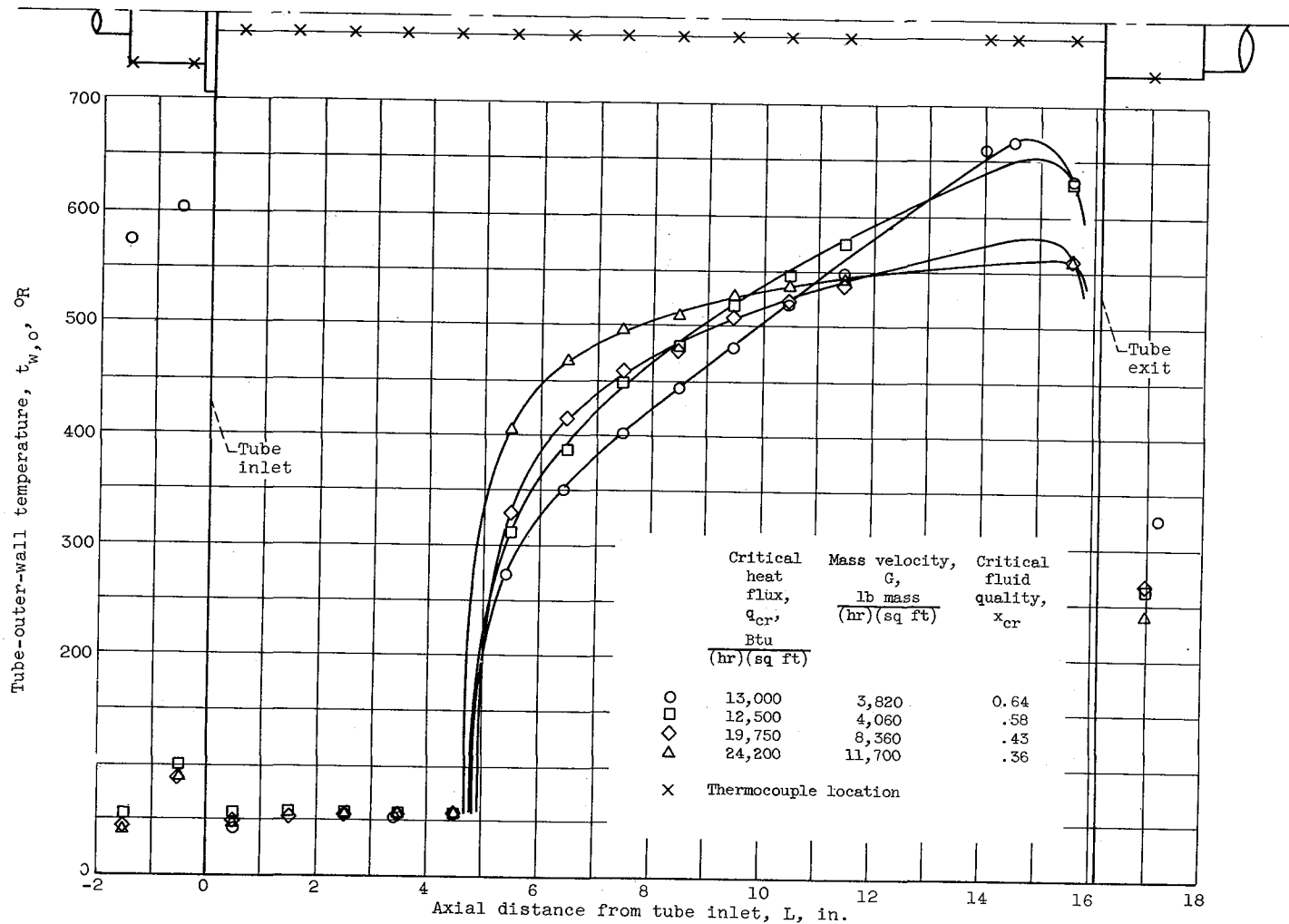


Figure 4. - Tube-outer-wall temperature profiles for flow of cool hydrogen gas through heated tube at several pressure, temperature, flow-rate, and heating-rate conditions.



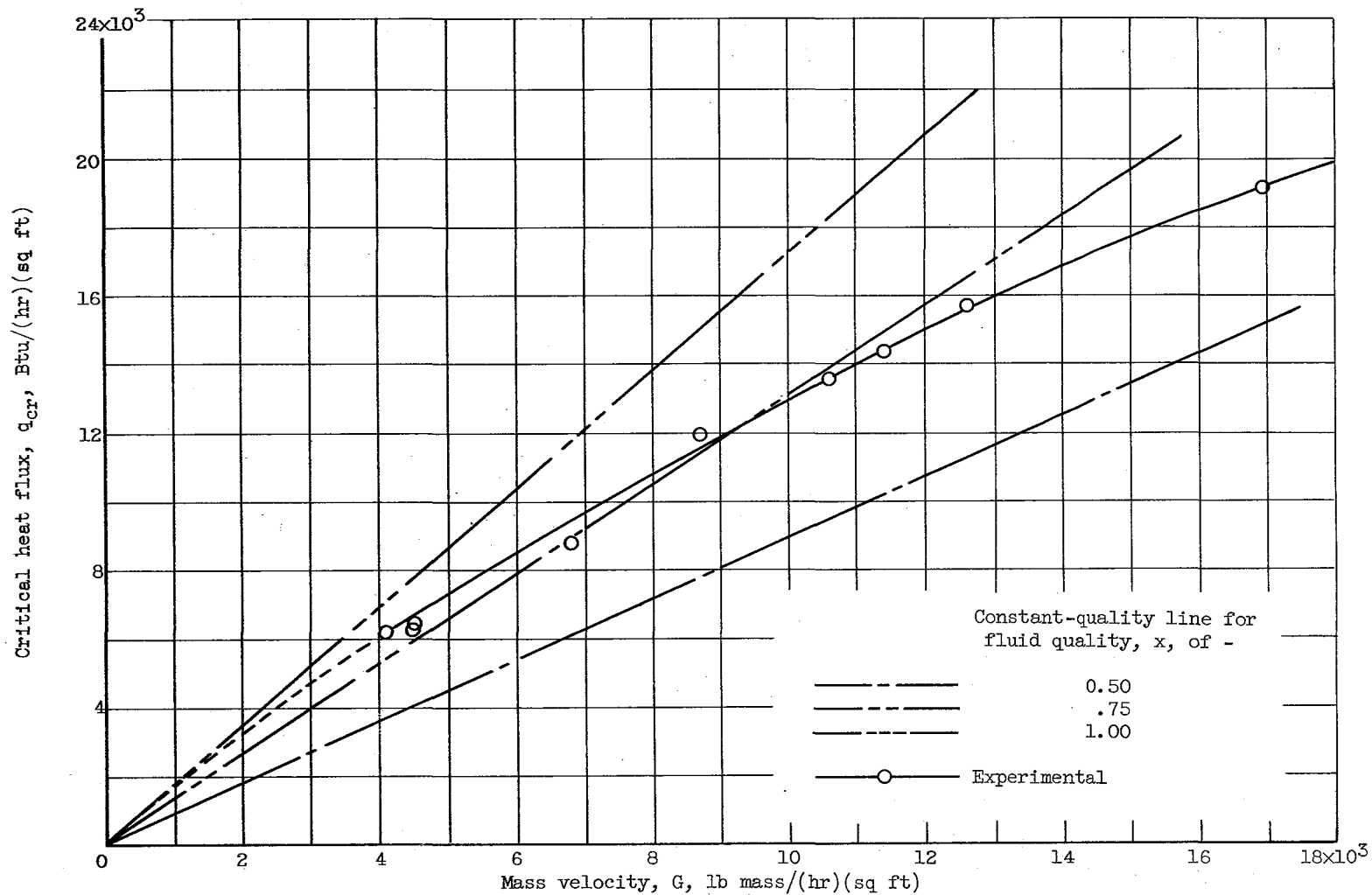
(a) Critical-boiling-length-to-diameter ratio, approximately 15.

Figure 5. - Tube-outer-wall temperature profiles for constant transition location and varying heat flux and mass velocity. Liquid hydrogen; test-section pressure, approximately 50 pounds per square inch absolute; average inlet subcooling, 2° R.



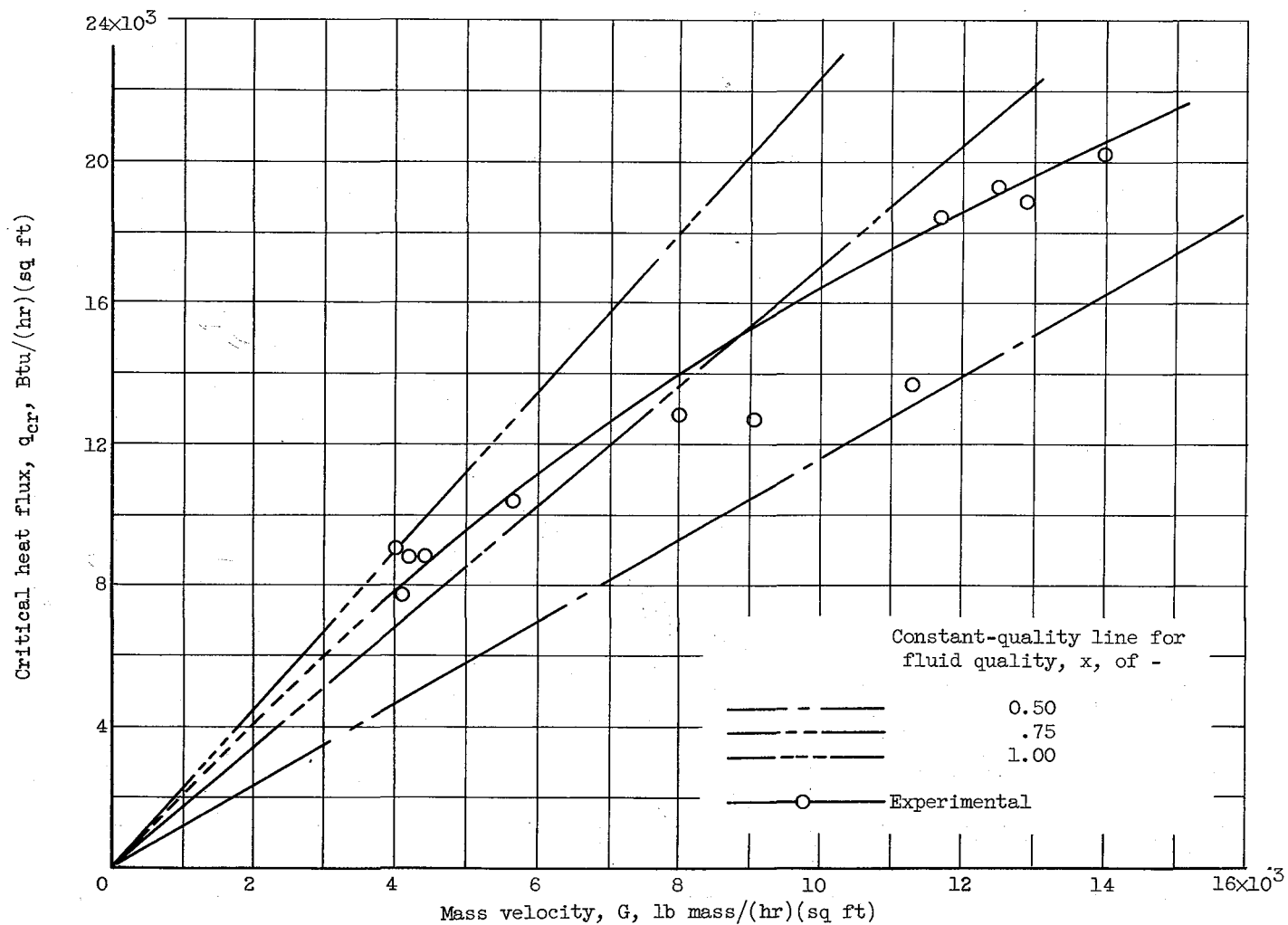
(b) Critical-boiling-length-to-diameter ratio, approximately 8.5.

Figure 5. - Concluded. Tube-outer-wall temperature profiles for constant transition location and varying heat flux and mass velocity. Liquid hydrogen; test-section pressure, approximately 50 pounds per square inch absolute; average inlet subcooling,  $2^{\circ}$  R.



(a) Critical-boiling-length-to-diameter ratio, approximately 26.

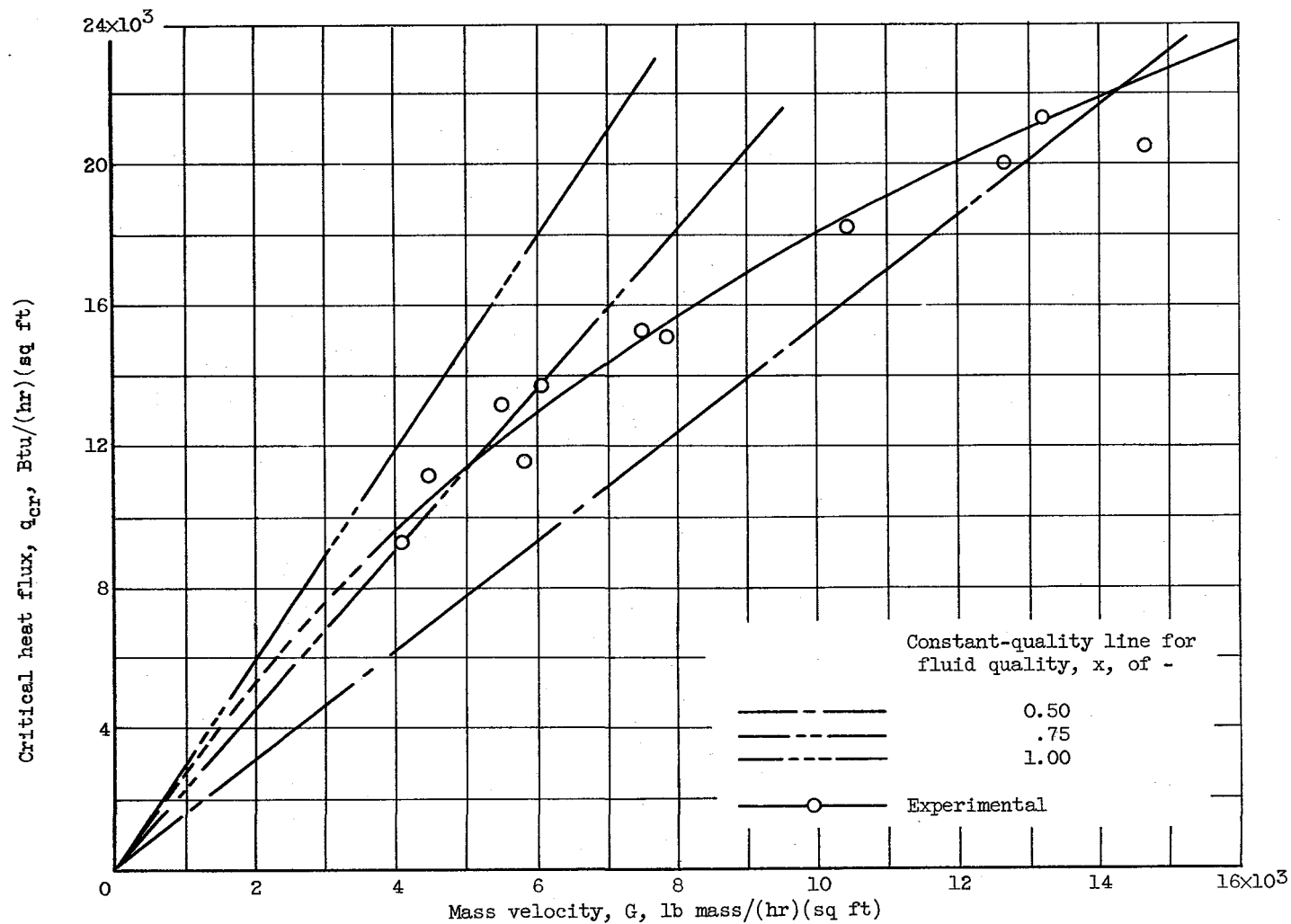
Figure 6. - Variation of critical heat flux with mass velocity. Liquid hydrogen; test-section pressure, approximately 50 pounds per square inch absolute; average inlet subcooling,  $2^\circ$  R.



(b) Critical-boiling-length-to-diameter ratio, approximately 20.

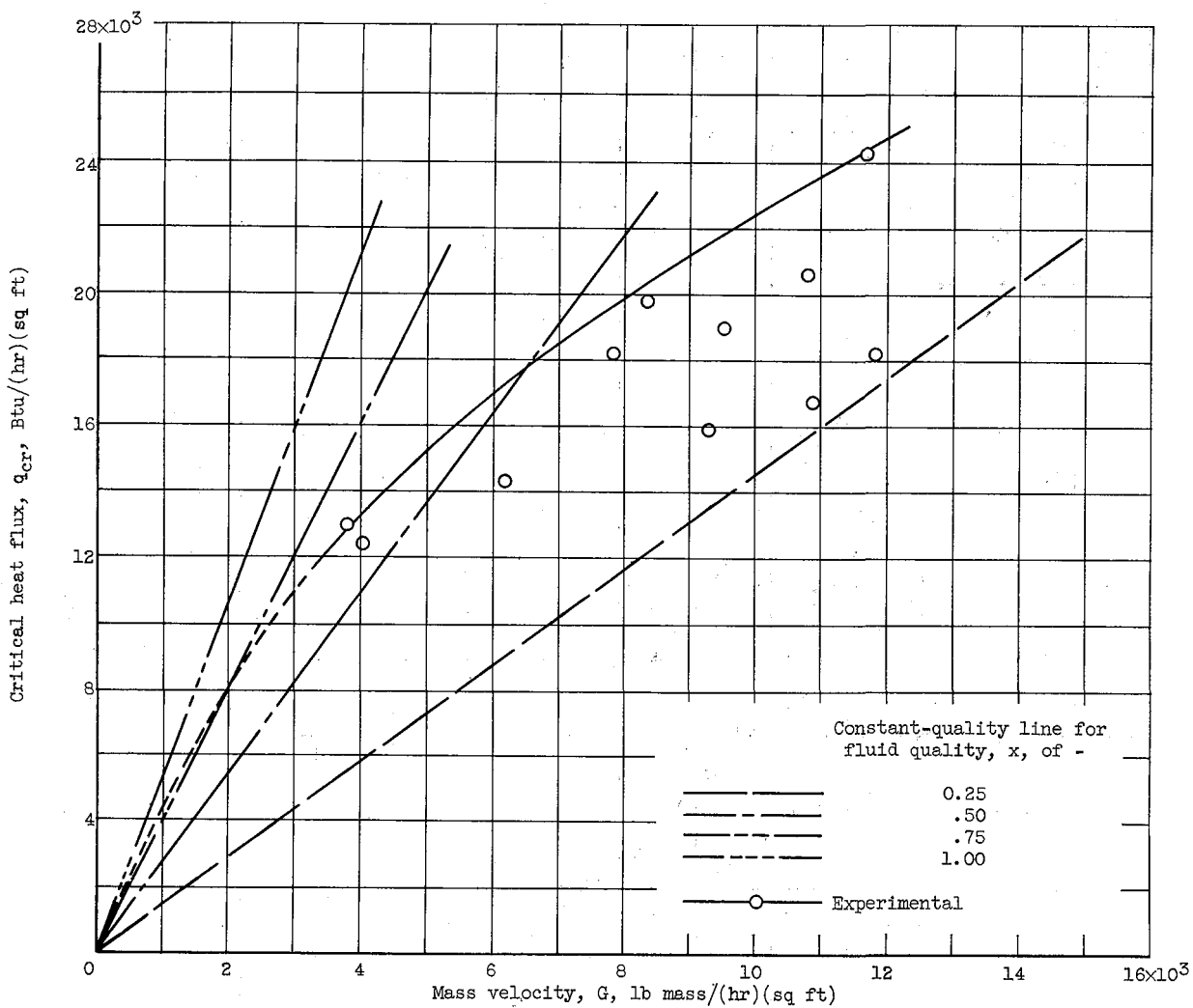
Figure 6. - Continued. Variation of critical heat flux with mass velocity. Liquid hydrogen; test-section pressure, approximately 50 pounds per square inch absolute; average inlet sub-cooling,  $2^\circ$  R.





(c) Critical-boiling-length-to-diameter ratio, approximately 15.

Figure 6. - Continued. Variation of critical heat flux with mass velocity. Liquid hydrogen; test-section pressure, approximately 50 pounds per square inch absolute; average inlet sub-cooling,  $2^\circ$  R.



(d) Critical-boiling-length-to-diameter ratio, approximately 8.5.

Figure 6. - Concluded. Variation of critical heat flux with mass velocity. Liquid hydrogen; test-section pressure, approximately 50 pounds per square inch absolute; average inlet sub-cooling,  $2^\circ \text{R}$ .

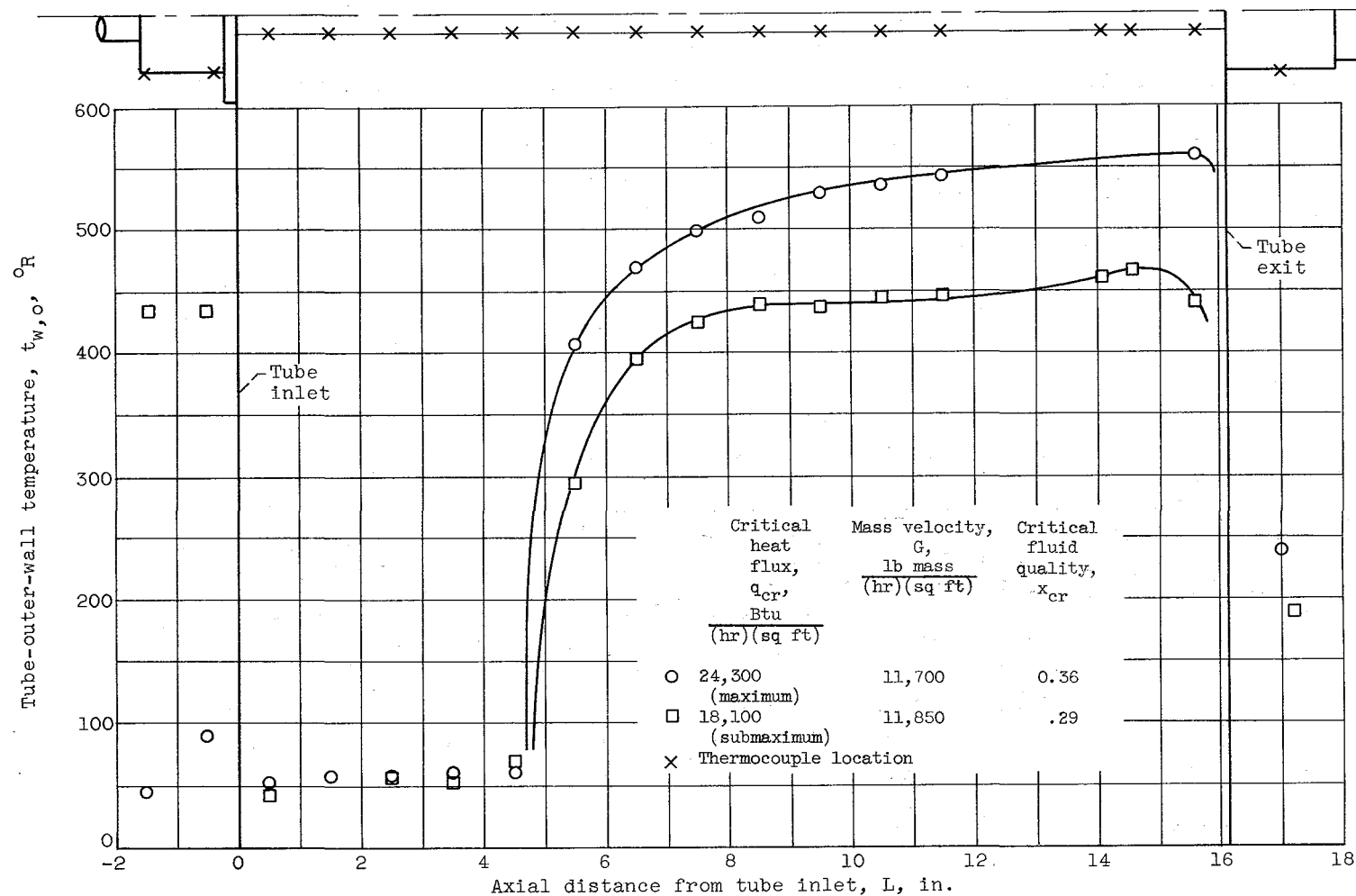


Figure 7. - Comparison of tube-outer-wall temperature profiles for maximum and submaximum critical-heat-flux conditions. Liquid hydrogen; test-section pressure, approximately 50 pounds per square inch absolute; average inlet subcooling,  $2^{\circ}\text{R}$ .

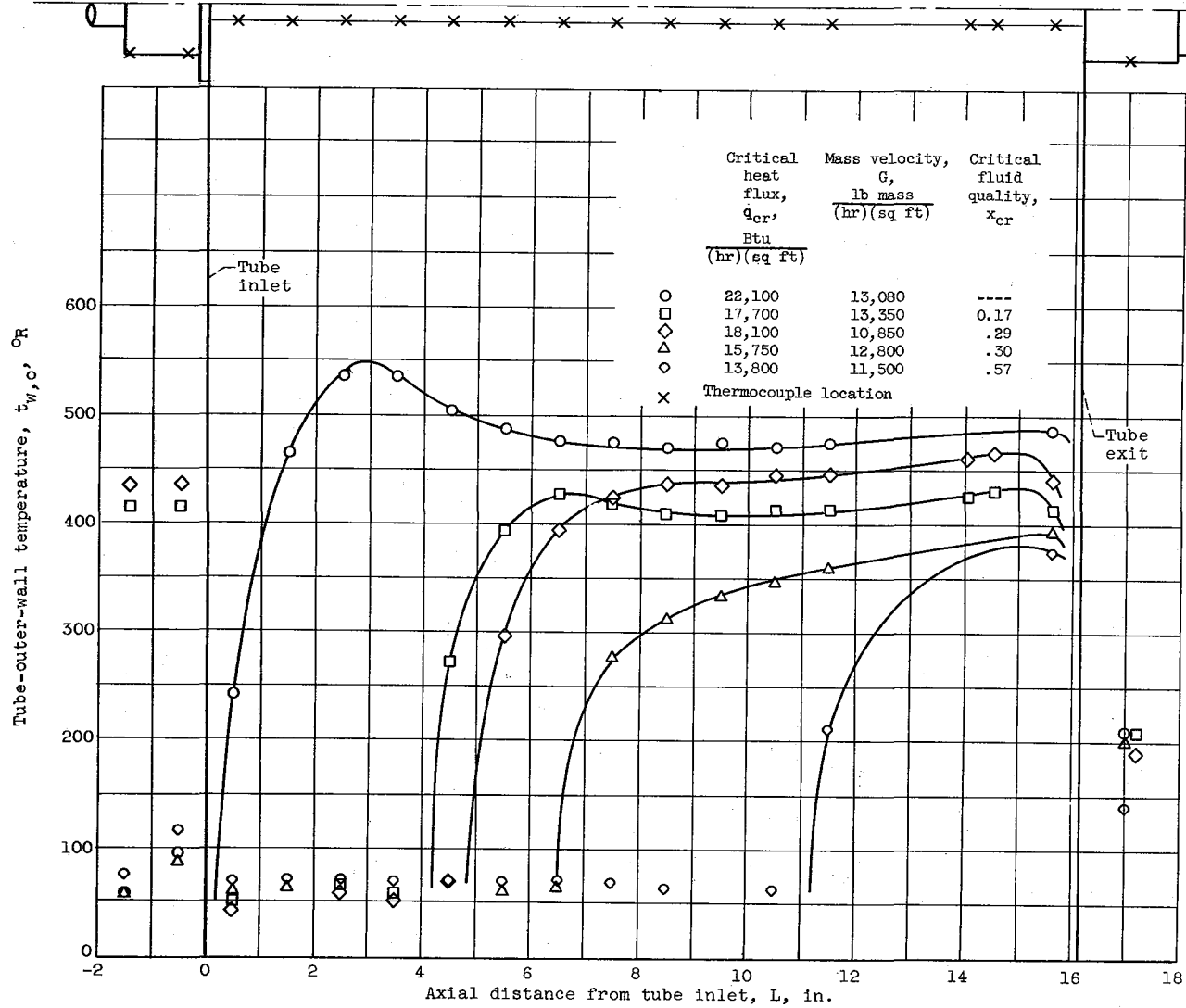
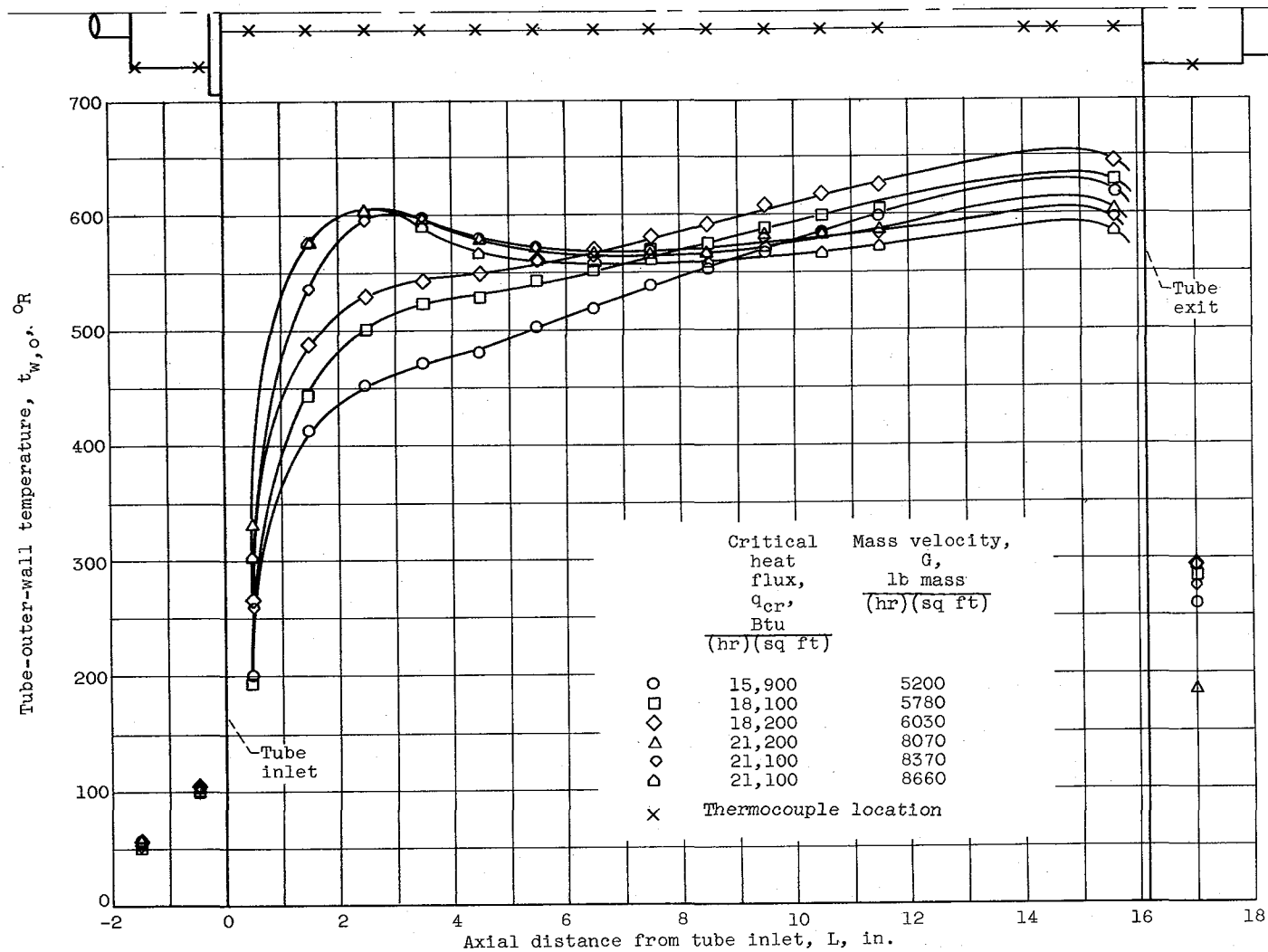
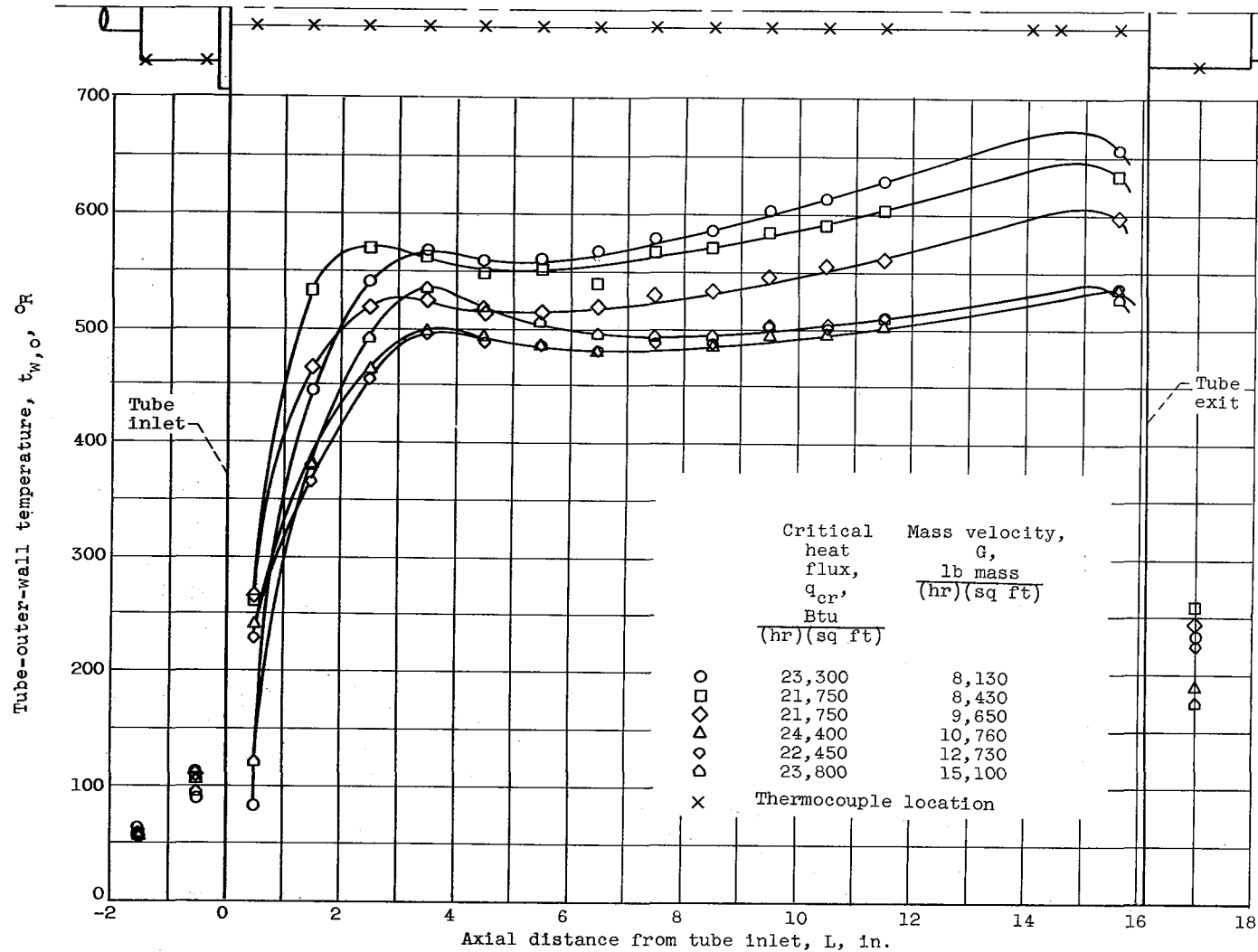


Figure 8. - Comparison of tube-outer-wall temperature profiles for submaximum critical-heat-flux conditions at various heat fluxes and constant mass velocity. Liquid hydrogen; test-section pressure, approximately 50 pounds per square inch absolute; average inlet subcooling, 2° R.



(a) Test-section pressure, approximately 50 pounds per square inch absolute.

Figure 9. - Tube-outer-wall temperature profiles for liquid hydrogen with wall temperature rise at tube inlet.



(b) Test-section pressure, approximately 70 pounds per square inch absolute.

Figure 9. - Concluded. Tube-outer-wall temperature profiles for liquid hydrogen with wall temperature rise at tube inlet.

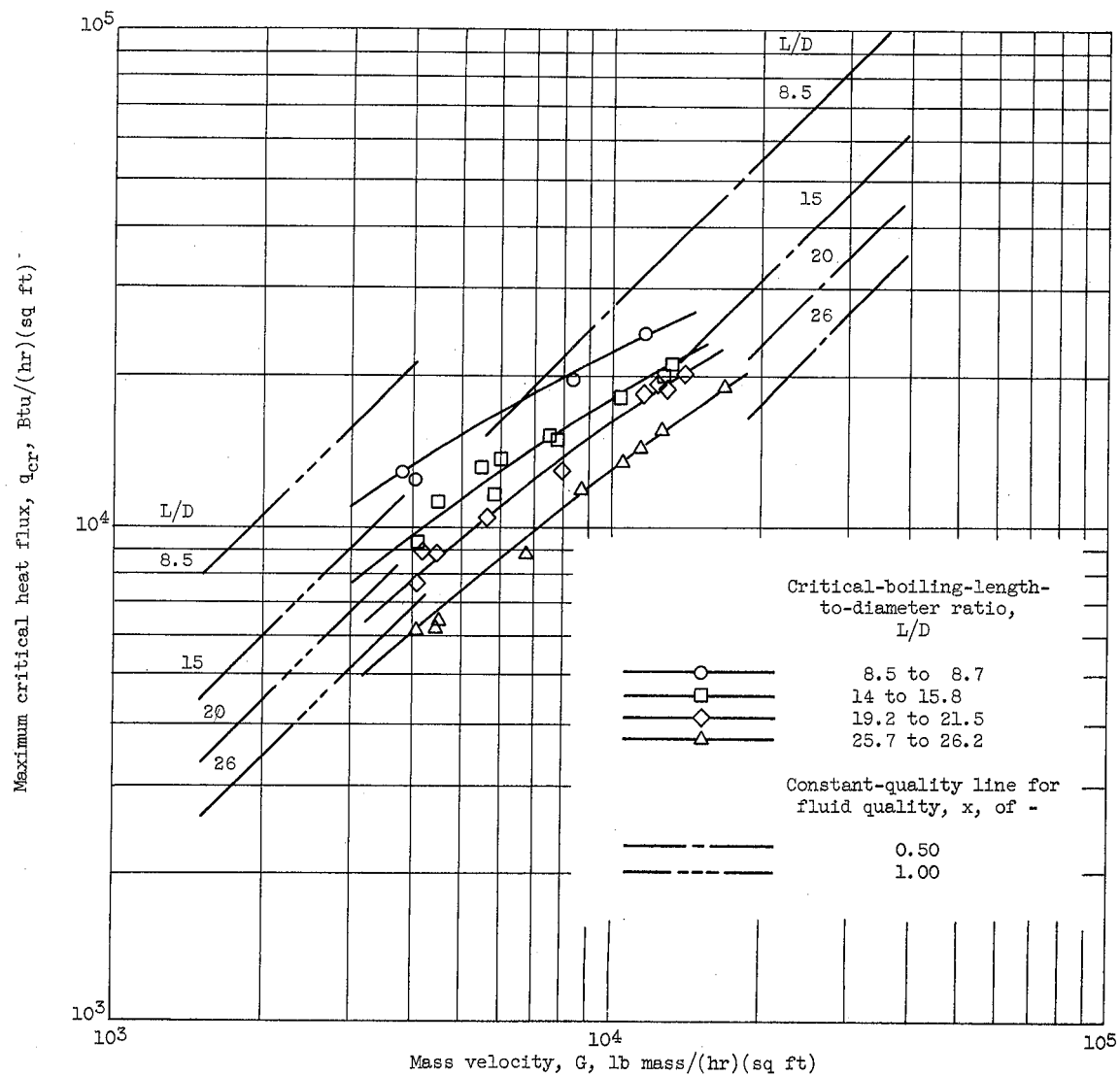


Figure 10. - Variation of maximum critical heat flux with mass velocity at various critical-boiling-length-to-diameter ratios. Liquid hydrogen; test-section pressure, approximately 50 pounds per square inch absolute; average inlet subcooling,  $2^{\circ}$  R.

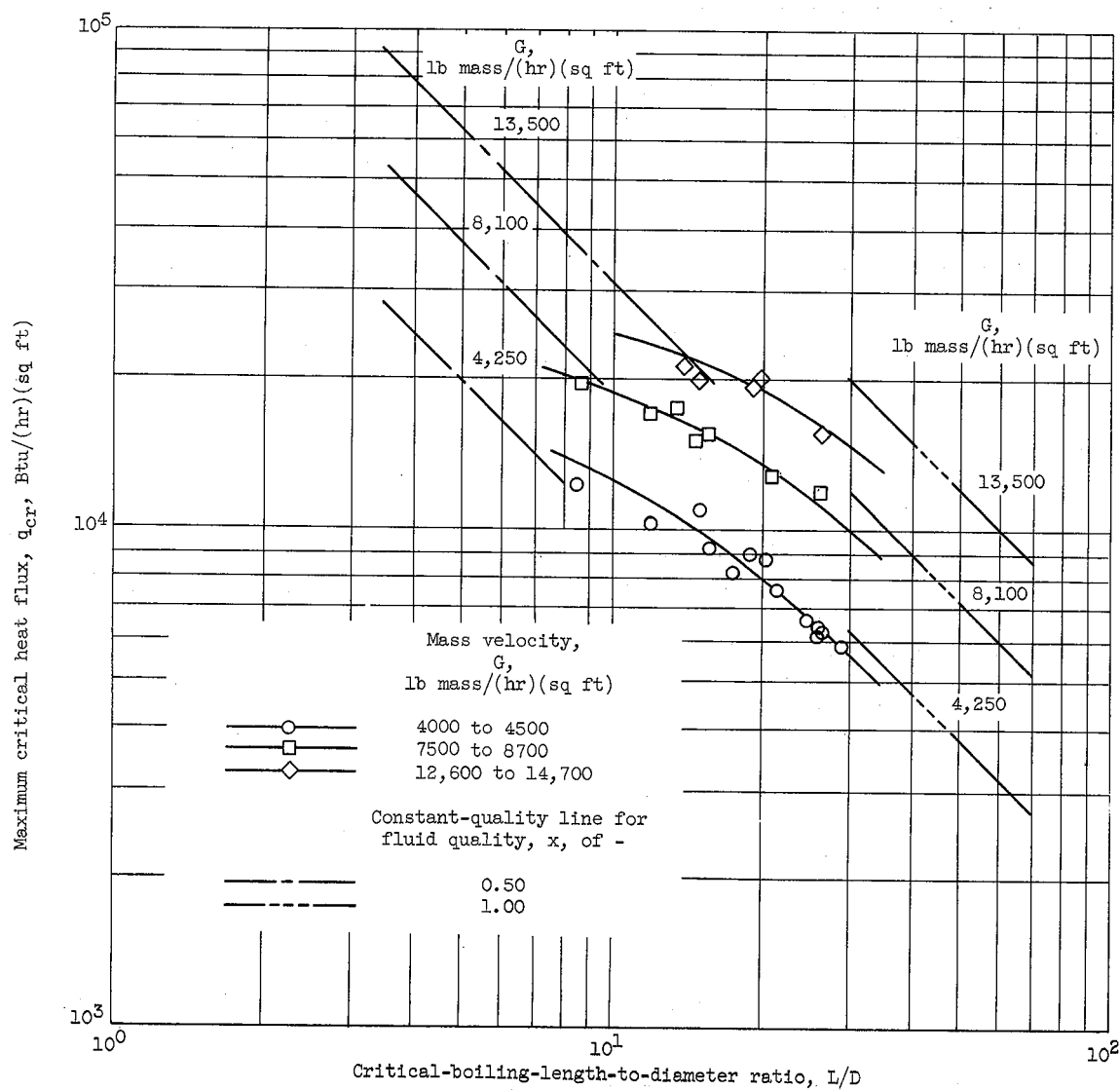


Figure 11. - Variation of maximum critical heat flux with critical-boiling-length-to-diameter ratio at various mass velocities. Liquid hydrogen; test-section pressure, approximately 50 pounds per square inch absolute; average inlet subcooling, 2° R.



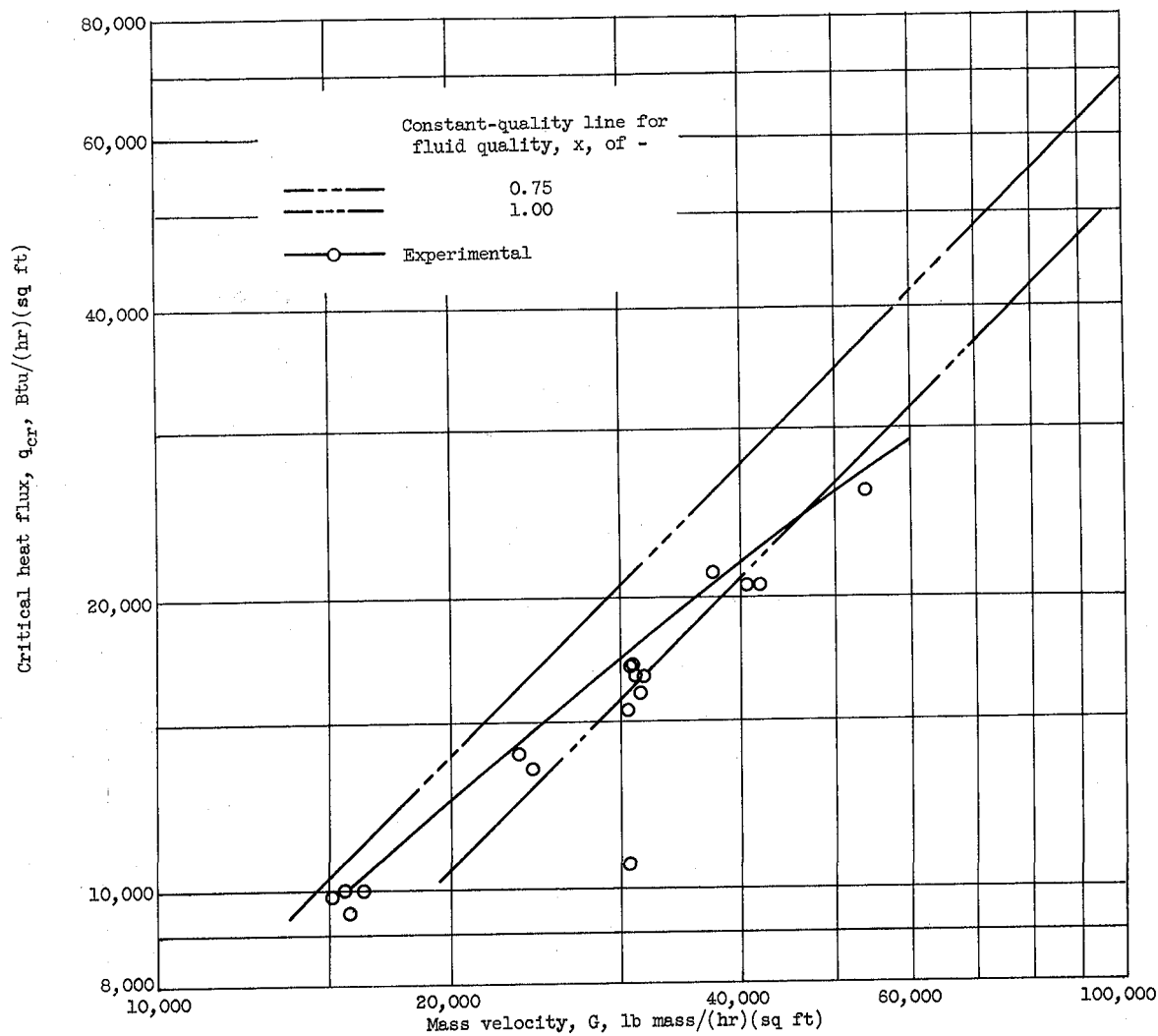


Figure 12. - Variation of critical heat flux with mass velocity at critical-boiling-length-to-diameter ratio of 29. Liquid nitrogen; test-section pressure, approximately 50 pounds per square inch absolute; average inlet subcooling,  $4^{\circ}$  R.

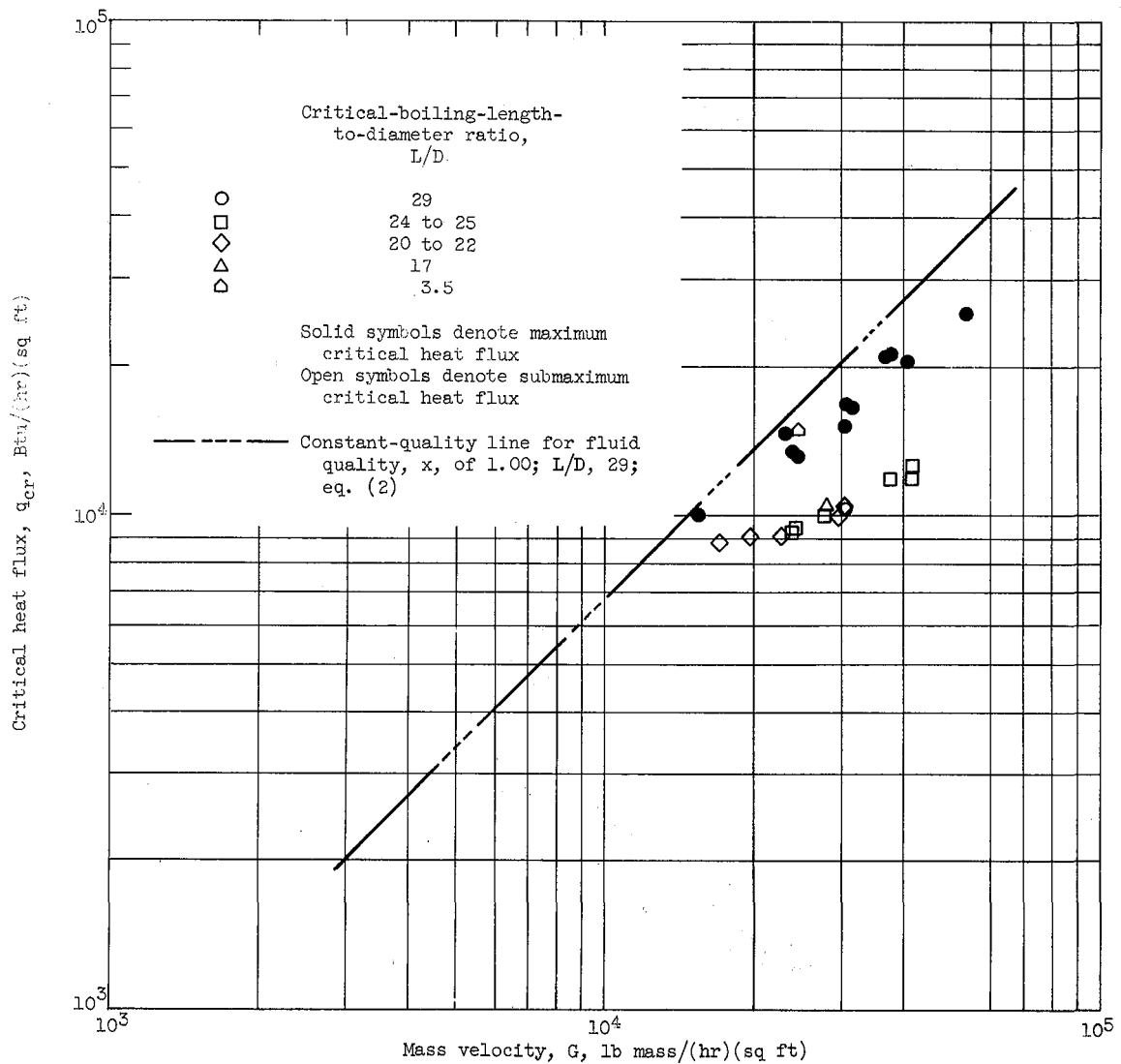


Figure 13. - Comparison of maximum critical boiling heat flux with submaximum critical boiling heat flux. Liquid nitrogen; test-section pressure, 48 to 53 pounds per square inch absolute; inlet subcooling,  $1^{\circ}$  to  $6^{\circ}$  R.

E-878

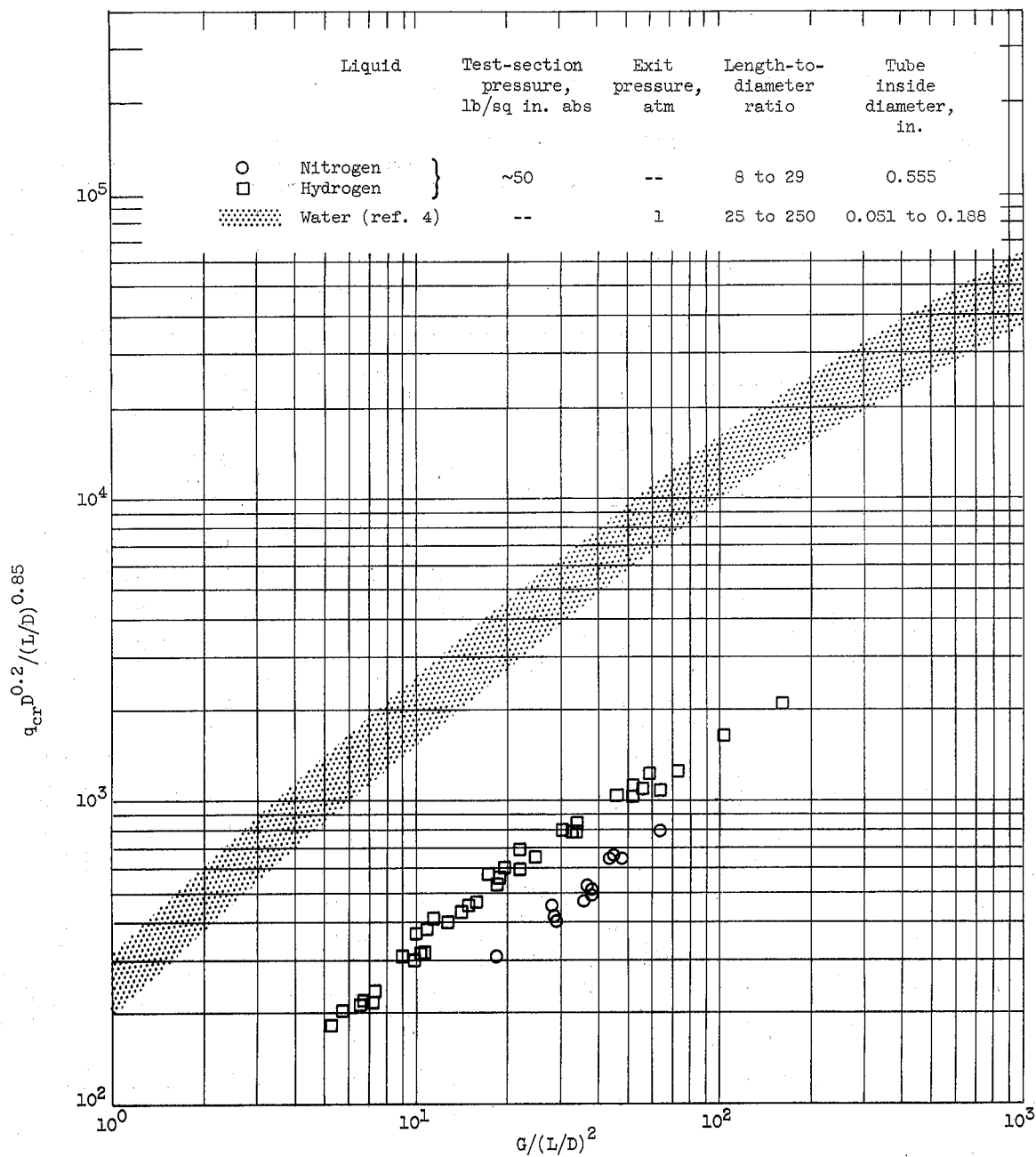


Figure 14. - Comparison of maximum critical heat flux for cryogenic liquids with water correlation of reference 4.

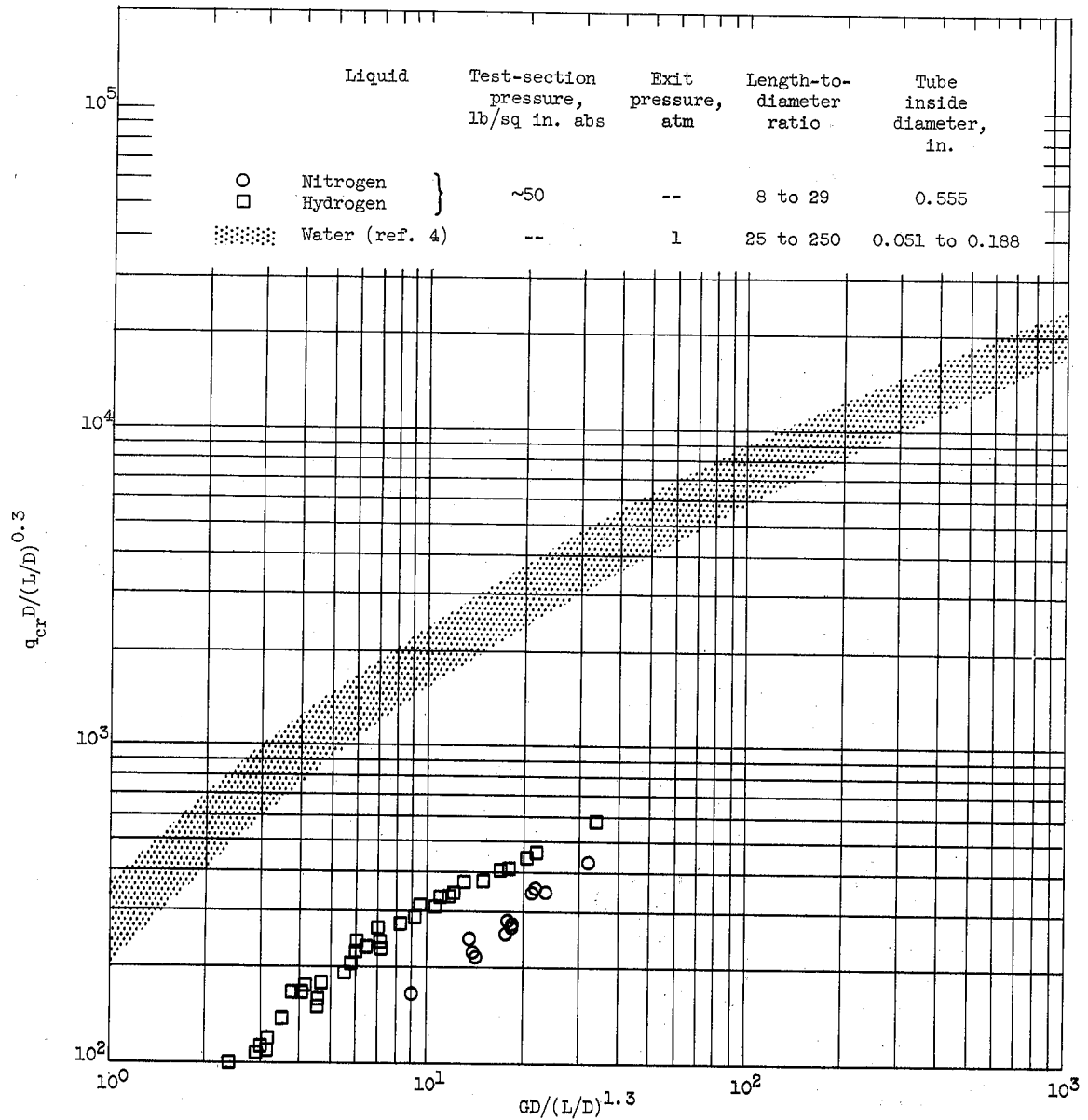


Figure 15. - Comparison of maximum critical heat flux for cryogenic liquids with water in terms of revised geometric parameters.

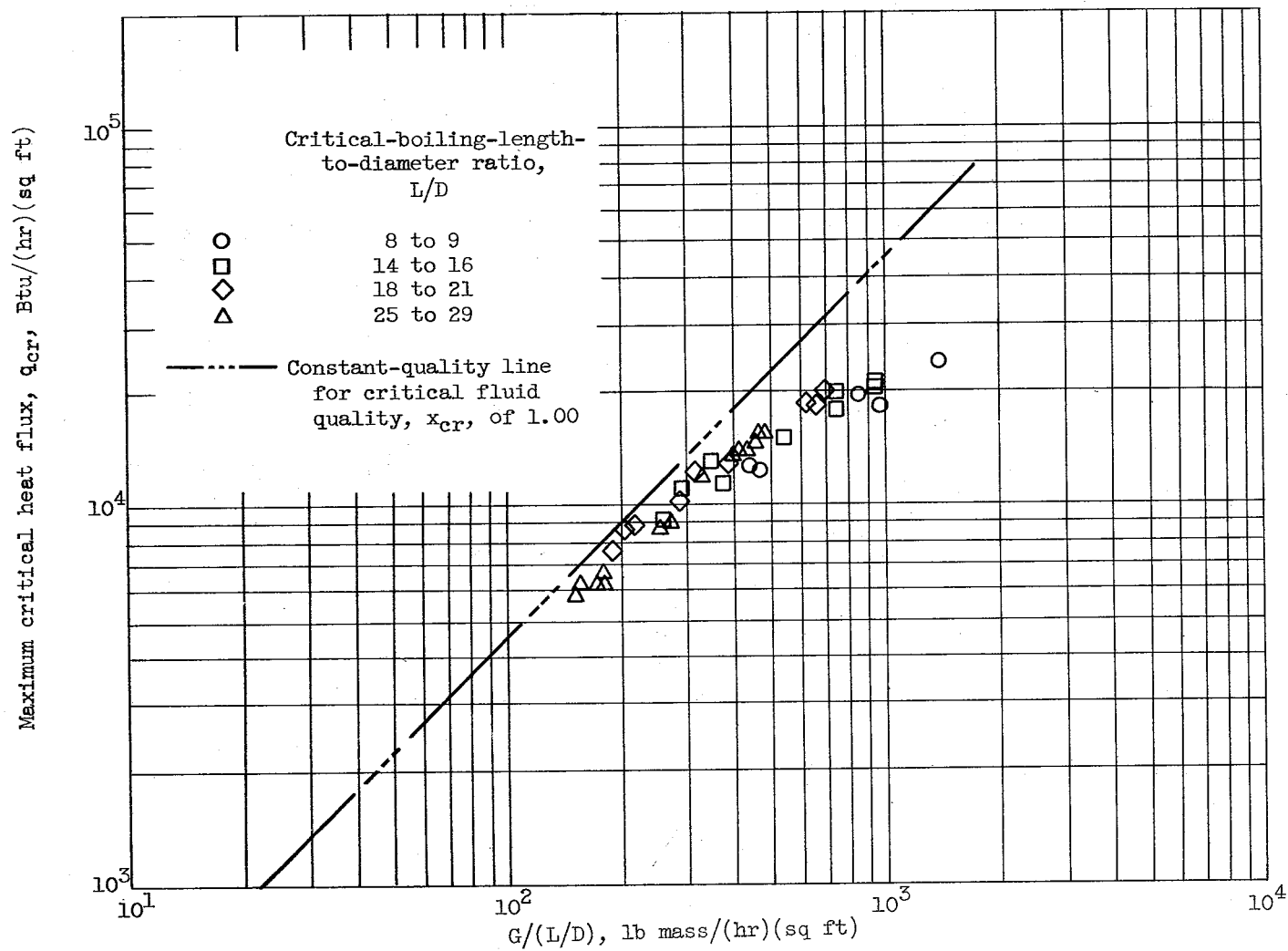


Figure 16. - Maximum critical heat flux as function of flow and length parameter. Boiling liquid hydrogen; tube inside diameter, 0.555 inch; test-section pressure, approximately 50 pounds per square inch absolute; average inlet subcooling,  $2^\circ$  R.

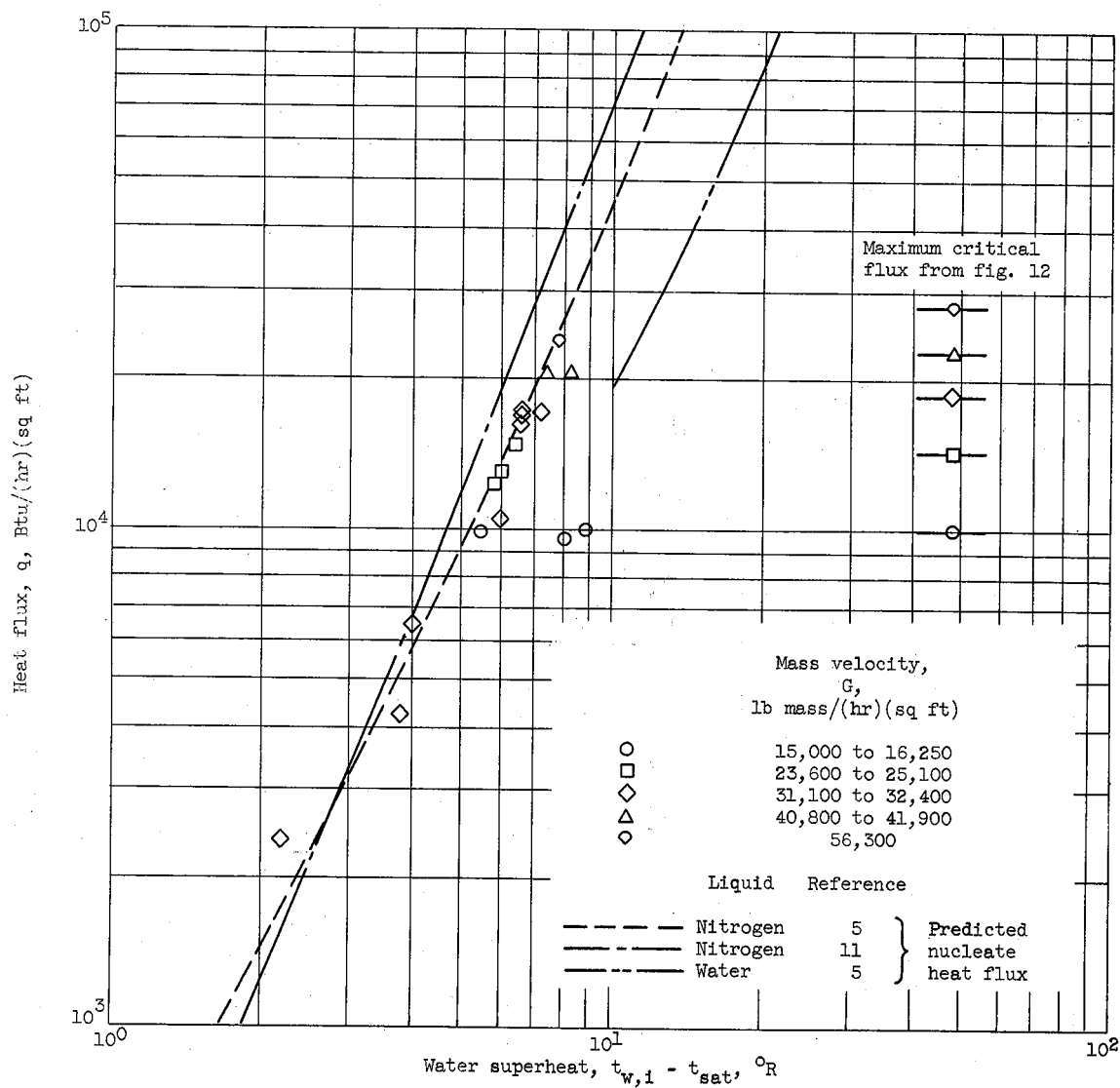


Figure 17. - Nucleate heat flux as function of wall superheat. Liquid nitrogen; test-section pressure, 48 to 56 pounds per square inch absolute; inlet subcooling, 3° to 5° R; length-to-diameter ratio, 29.

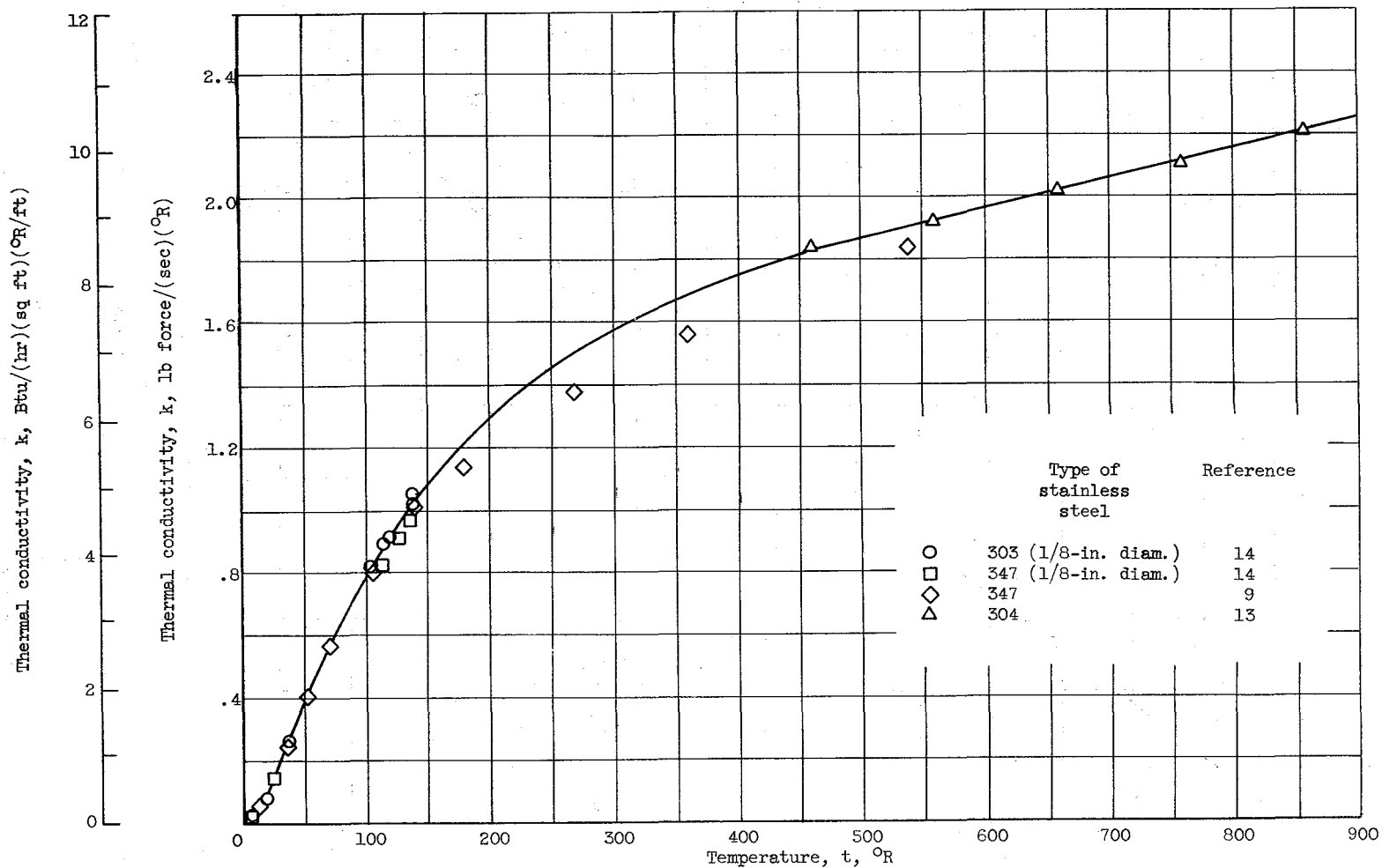


Figure 18. - Variation of thermal conductivity of 303, 304, and 347 stainless steel with temperature.

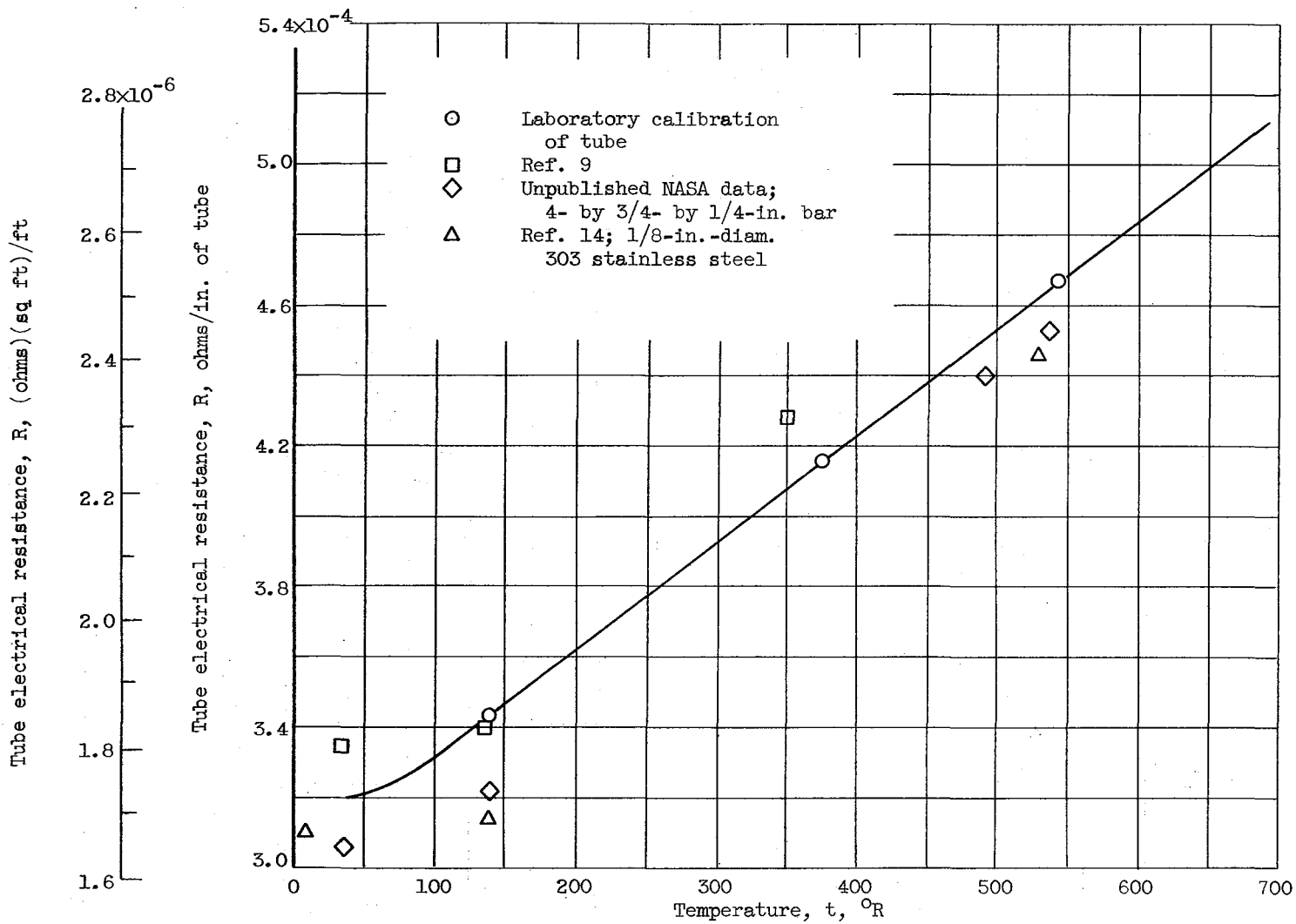


Figure 19. - Variation of tube electrical resistance with temperature. Tube of 304 stainless steel; outside diameter, 0.625 inch; inside diameter, 0.555 inch.



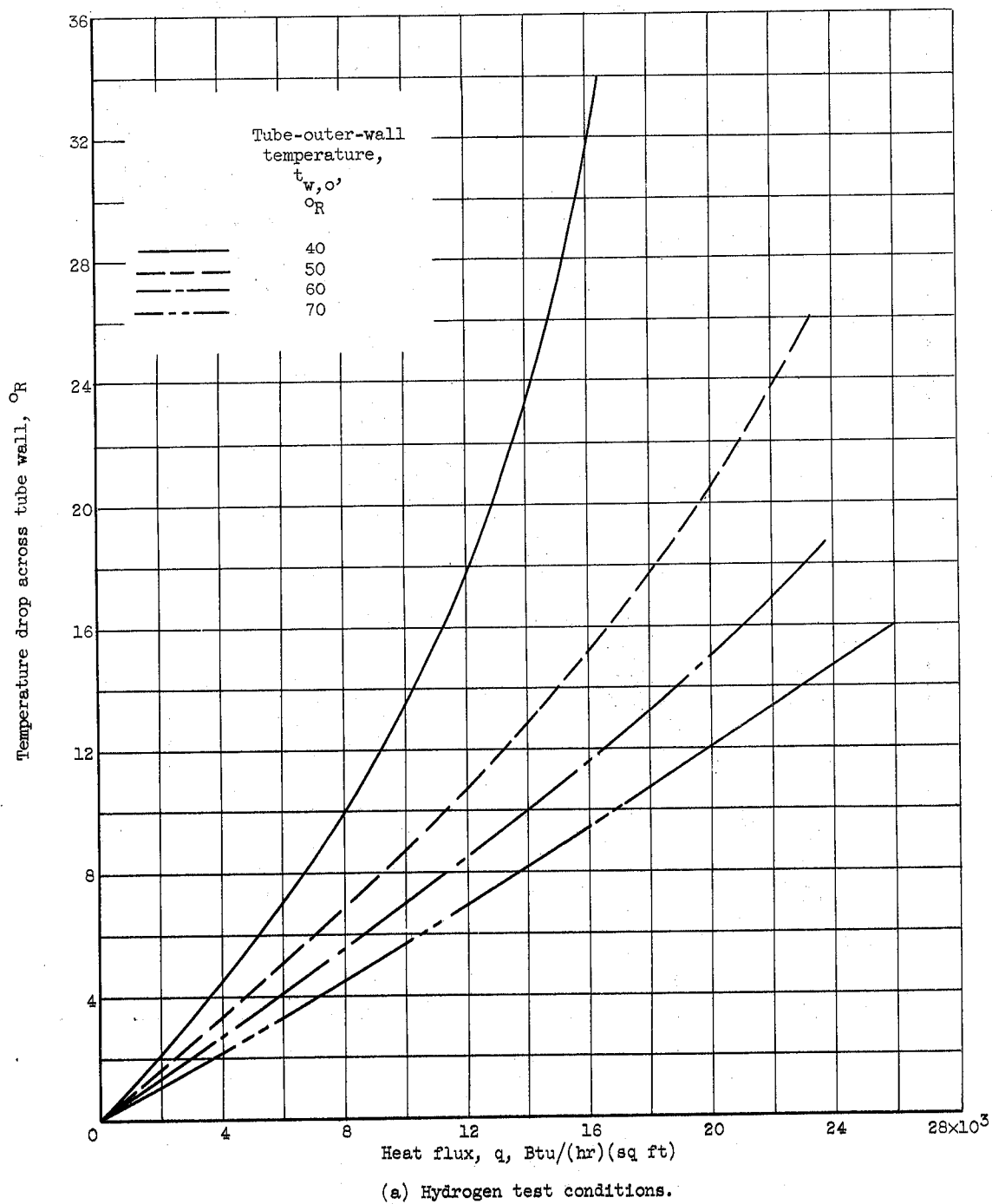
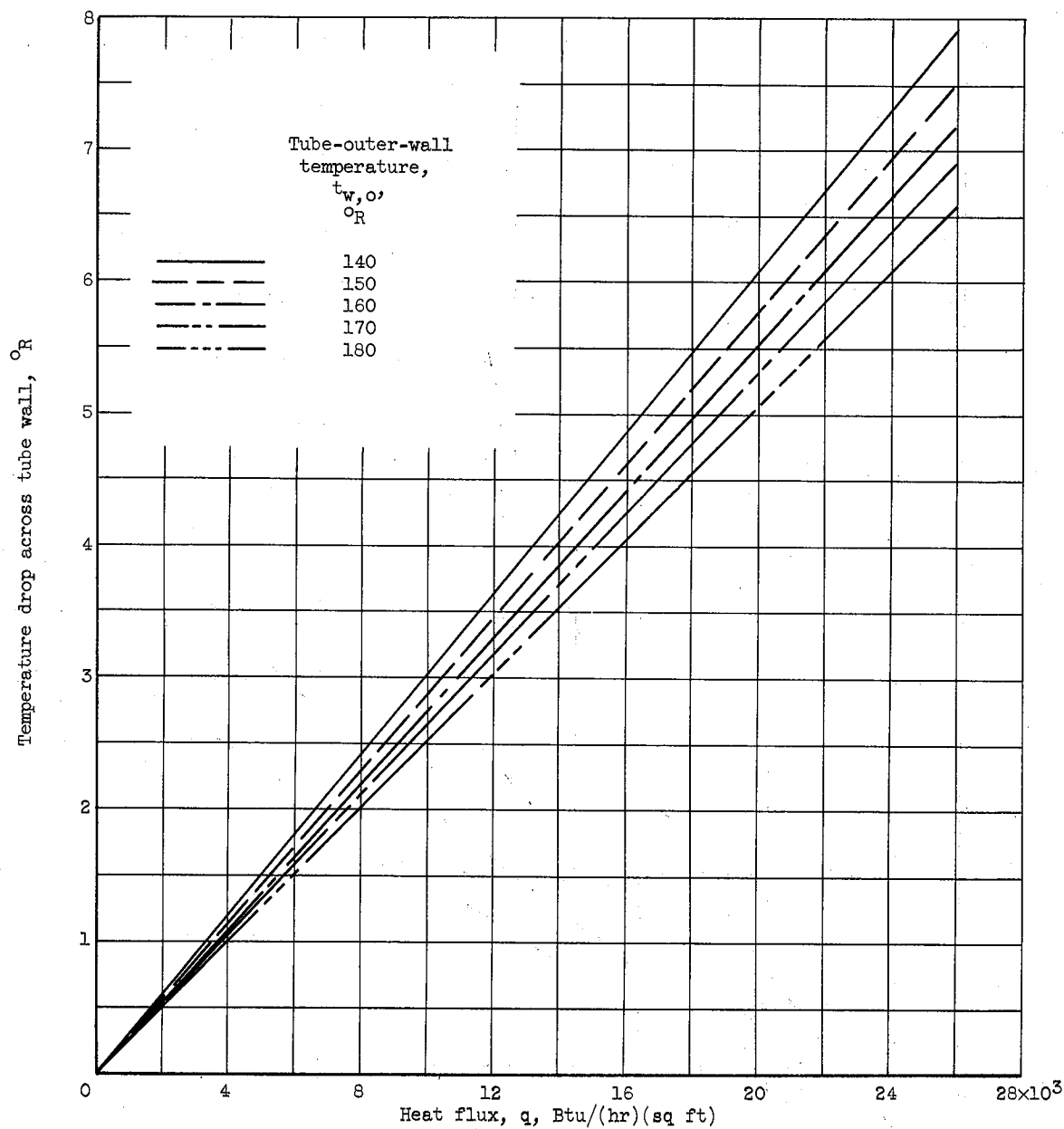


Figure 20. - Temperature drop across tube wall as function of heat flux and tube-outer-wall temperature. Negligible axial temperature gradient; tube of 304 stainless steel; inside diameter, 0.555 inch; wall thickness, 0.035 inch.



(b) Nitrogen test conditions.

Figure 20. - Concluded. Temperature drop across tube wall as function of heat flux and tube-outer-wall temperature. Negligible axial temperature gradient; tube of 304 stainless steel; inside diameter, 0.555 inch; wall thickness, 0.035 inch.